Journal of Paleontology, 97(6), 2023, p. 1251–1281

Published by Cambridge University Press
on behalf of The Paleontological Society
0022-3360/23/1937-2337
doi: 10.1017/jpa.2023.58

JOURNAL OF PALEONTOLOGY
A PUBLICATION OF THE Paleontological SOCIETY

A new eryopid temnospondyl from the Carboniferous–Permian boundary of Germany

Ralf Werneburg,[1]* Florian Witzmann,[2] Larry Rinehart,[3] Jan Fischer,[4] and Sebastian Voigt[4]

[1]Naturhistorisches Museum Schloss Bertholdsburg Schleusingen, Burgstrasse 6, D-98553 Schleusingen, Germany. <werneburg@museum-schleusingen.de>
[2]Museum für Naturkunde, Leibniz Institute for Evolution and Biodiversity Science, Invalidenstraße 43, D-10115 Berlin, Germany. <florian.witzmann@mfn.berlin>
[3]New Mexico Museum of Natural History, 1801 Mountain Road NW, Albuquerque, NM 87104, USA. <larry.rinehart@earthlink.net>
[4] Urweltmuseum GEOSKOP/Burg Lichtenberg (Pfalz), Burgstrasse 19, 66871 Thallichtenberg, Germany. <j.fischer@pfalzmuseum.bv-pfalz.de>, <s.voigt@pfalzmuseum.bv-pfalz.de>

Non-technical Summary.—The new fossil eryopid amphibian *Stenokranio boldi*, a temnospondyl closely related to *Eryops*, is described here. The new crocodile-like amphibian is based on well-preserved cranial and postcranial material from ca. 300 million-year-old fluvio-lacustrine deposits of the Permo-Carboniferous (Gzhelian/Asselian) in the Saar–Nahe Basin of southwestern Germany. Phylogenetic analysis identifies *Stenokranio* as a sister taxon to *Eryops*. *Stenokranio* was among the largest predators of the Saar–Nahe Basin. Due to its semiaquatic lifestyle, *Stenokranio* was able to scour the river and lake shores for prey, but most likely fed on aquatic vertebrates. *Stenokranio* was part of a faunal assemblage of aquatic, semiaquatic, and fully terrestrial vertebrates, such as sarcopterygian and actinopterygian fishes, xenacanthid sharks, a dvinosaurian temnospondyl, and various other tetrapods ("lepospondyls", diadectomorphs, and synapsids). This corresponds broadly to the vertebrate community from Permo-Carboniferous rocks in North America that are approximately the same age.

Abstract.—A new eryopid temnospondyl, *Stenokranio boldi* n. gen. n. sp. is described based on well-preserved cranial and postcranial material from fluvio-lacustrine deposits of the Permo-Carboniferous (Gzhelian/Asselian) Remigiusberg Formation at the Remigiusberg quarry near Kusel, Saar–Nahe Basin, southwest Germany. The new taxon is characterized by three autapomorphies within the Eryopidae: (1) the relatively narrow posterior skull table, therefore nearly parallel lateral margins of the skull; (2) the short postparietals and tabulars; and (3) the wide ectopterygoid. Phylogenetic analysis reveals a monophyletic Eryopidae with the basal taxa *Osteophorus*, *Glaukerpeton*, and *Onchiodon labyrinthicus* forming a polytomy. *Actinodon* may be either a basal eryopid or a stereospondylomorph, and the genus *Onchiodon* is not monophyletic. *Stenokranio* n. gen. is found as a more derived eryopid forming the sister taxon to *Eryops*. *Stenokranio* n. gen. was among the largest predators of the Saar–Nahe Basin. Its semiaquatic lifestyle enabled *Stenokranio* n. gen. to browse riverbanks and lake shorelines for prey, but most likely it fed on aquatic vertebrates. *Stenokranio* n. gen. was part of a faunal assemblage of aquatic, semiaquatic, and fully terrestrial vertebrates, such as sarcopterygian and actinopterygian fishes, xenacanthid sharks, a dvinosaurian temnospondyl, different "lepospondyls", diadectomorphs, and synapsids. This is in general accordance with the vertebrate community from the Permo-Carboniferous of North America and from the early Permian localities of Manebach (Thuringian Forest Basin) and Niederhäslich (Döhlen Basin). It is notable that the occurrence of *Stenokranio* n. gen. and other eryopids in these localities excluded the presence of other large temnospondyls such as *Sclerocephalus*. However, a previously described isolated eryopid mandible from the Remigiusberg locality differs from that of *Stenokranio* n. gen. in several characters, implying that probably two different eryopid taxa lived at the same locality.

UUID: www.zoobank.org/88a52547-d6fc-40af-965c-a6786c252ed5

Introduction

Eryopids are widespread nonmarine temnospondyl amphibians that are especially well known from large representatives of the genus *Eryops* Cope, 1878, from the latest Carboniferous and early Permian rocks of the United States (Cope, 1882; Case, 1911; Miner, 1925; Sawin, 1941; Pawley and Warren, 2006; Werneburg et al., 2010). Eryopids were a conspicuous component of the North American early Permian tetrapod assemblage, which included aquatic temnospondyls and terrestrial diadectids, edaphosaurids, and sphencacodontids. Eryopids had a wide geographical distribution on northern Pangea, from the well-known occurrences of North America up to the eastern

*Corresponding author.

margin of Europe, with several European localities, including Germany (Werneburg, 1987; Boy, 1990; Schoch and Hampe, 2004; Witzmann, 2013; Witzmann and Voigt, 2014), France (Werneburg, 1997; Werneburg and Steyer, 1999), Czech Republic (Werneburg, 1993), Poland (Meyer, 1860a), and Russia (Gubin, 1983).

This work focuses on eryopid remains found in fluvio-lacustrine deposits of the latest Carboniferous–earliest Permian (Gzhelian/Asselian) Remigiusberg Formation at the Remigiusberg quarry near Kusel, Saar–Nahe Basin, southwest Germany, in 2013–2018 (Voigt et al., 2014, 2019). The incomplete, but excellently preserved material, including two skulls, is interpreted to represent a new species and new genus. The new eryopid of the Saar–Nahe Basin is one of the stratigraphically oldest eryopids of Europe and among the oldest eryopids in the world. The closest in age is the European temnospondyl *Onchiodon thuringiensis* Werneburg, 2007, from the earliest Asselian of the Thuringian Forest Basin, central Germany (Werneburg, 2007), but this form shows many differences from the new eryopid. Apart from the anatomical description and taxonomic and phylogenetic analyses of the new eryopid from SW Germany, this contribution stimulates the reevaluation of eryopid paleoecology as a whole.

Geological setting and age

All of the eryopid material described herein comes from the Remigiusberg quarry near Kusel, Rhineland–Palatinate, SW-Germany (Fig. 1). The Remigiusberg quarry belongs to the continental Carboniferous–Permian Lorraine–Saar–Nahe Basin, which is one of the largest intramontane basins of the European Variscides (Schäfer, 1986). Because the French part of the basin fill is mainly covered by younger sediments, regional geologists often talk merely of the Saar–Nahe Basin referring to an area of about 40 × 120 km in SW Germany where Carboniferous–Permian rocks almost continuously crop out (Boy et al., 2012). The Saar–Nahe Basin accumulated an up to a 10,000-m-thick succession of volcano-sedimentary rocks between early late Carboniferous (Bashkirian) and supposed middle to late early Permian (Artinskian–Kungurian) time (Schneider et al., 2020; Menning et al., 2022).

The Remigiusberg quarry is a large, active, open-cast mine, producing subvolcanic rock for the production of road and railroad gravel. Subvolcanic rock of the quarry is derived from a sill-like early Permian (Asselian–Sakmarian) intrusion into mainly siliciclastic rocks of the latest Carboniferous to earliest Permian (Gzhelian–Asselian) Remigiusberg Formation. Up to 40 m of fluvio-lacustrine and deltaic sediments of the Remigiusberg Formation currently exposed at the Remigiusberg quarry show a complex interbedding of fluvio-deltaic conglomerate, sandstone, and mudstone, with lacustrine limestone and volcanic tuff beds as minor components. Lithostratigraphic subdivision of the succession is based on seven limestone units ranging 20–150 cm in thickness. The limestone units are referred to the Theisbergstegen and Haschbach lake levels of the middle part and to the Friedelhausen lake level of the basal upper part of the Remigiusberg Formation (Boy and Schindler, 2000; Fröbisch et al., 2011; Boy et al., 2012; Voigt et al., 2014, 2019; Fig. 2). Radioisotopic dates from volcanic tuff beds of the Remigiusberg and immediately overlying Altenglan formations suggest that the sediments exposed at the Remigiusberg quarry cover the Carboniferous–Permian boundary with a

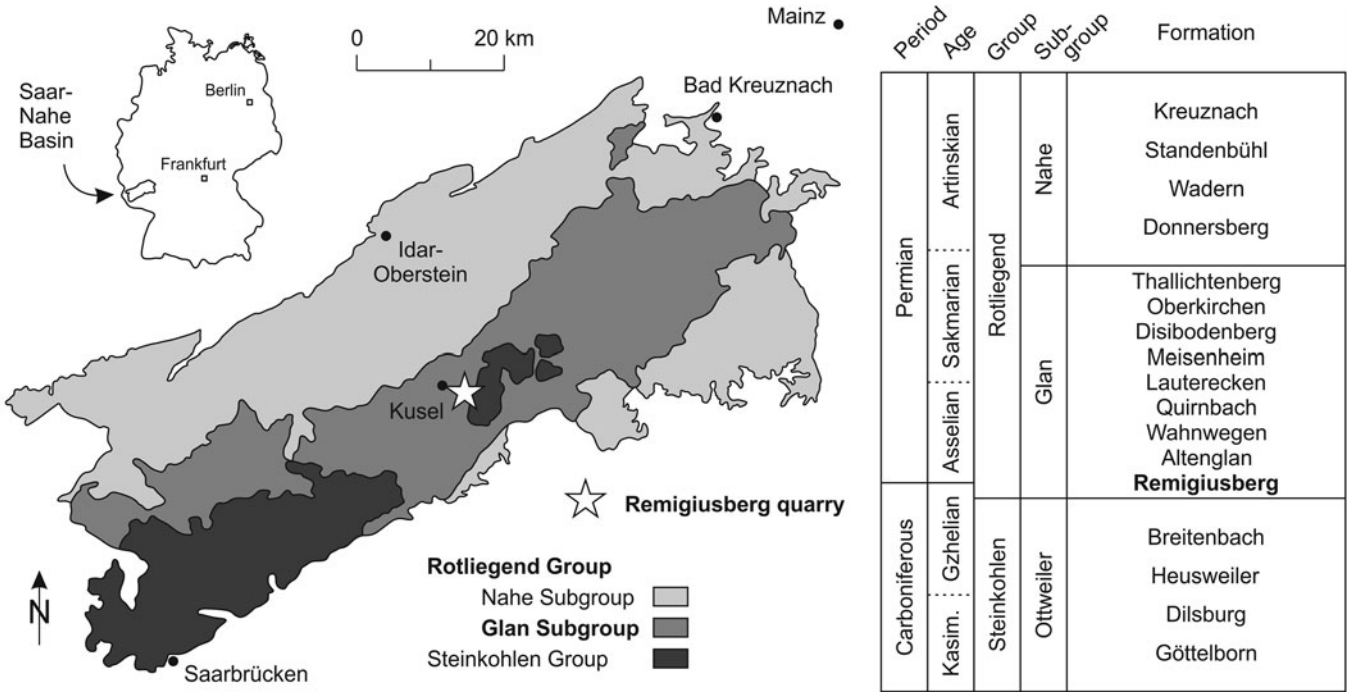

Figure 1. Simplified geological map and lithostratigraphic subdivision of the post-Moscovian part of the Carboniferous–Permian volcano-sedimentary succession of the Saar–Nahe Basin (adapted from Stapf, 1990, Boy et al., 2012; correlation of formation boundaries with the chronostratigraphic timescale based on Schneider et al., 2020). The type locality of *Stenokranio boldi* n. gen. n. sp. in the Remigiusberg Formation at the Remigiusberg quarry near Kusel is marked by a star.

https://doi.org/10.1017/jpa.2023.58 Published online by Cambridge University Press

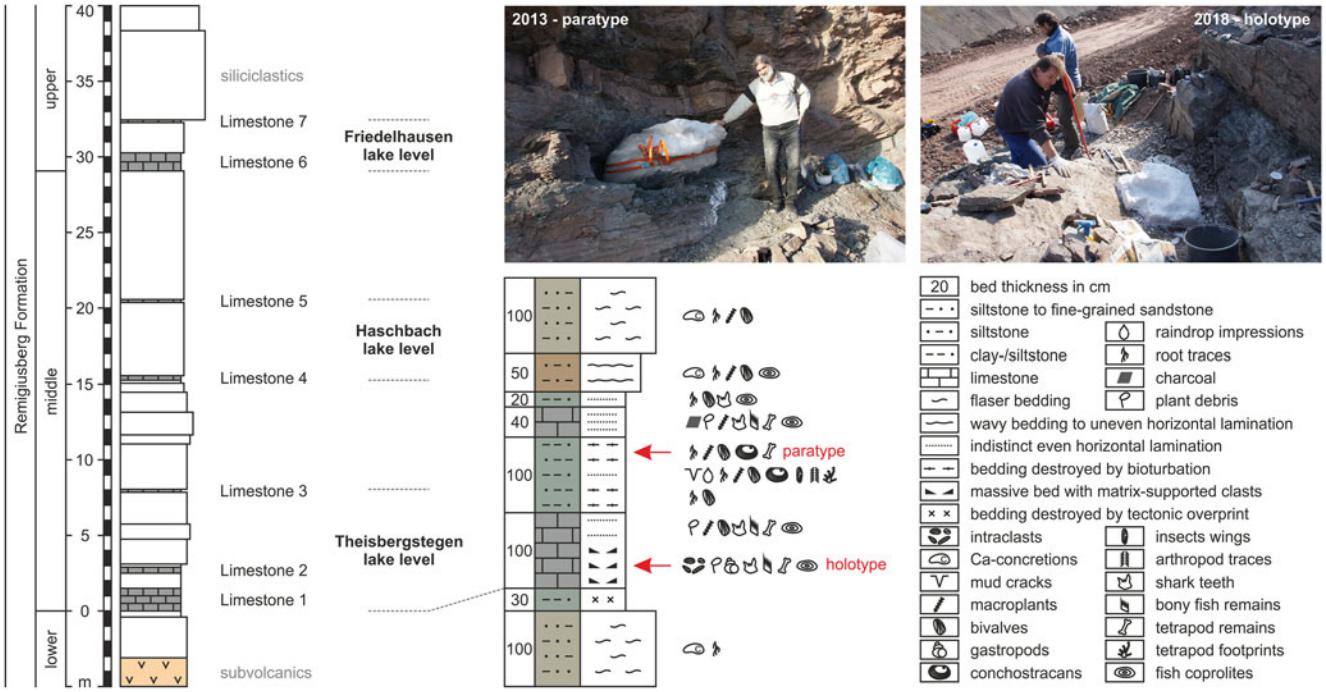

Figure 2. Lithostratigraphy of the Remigiusberg Formation at the Remigiusberg quarry near Kusel and detailed section of the lower Theisbergstegen lake level at the type locality of *Stenokranio boldi* n. gen. n. sp.

minimum age of 298.7 ± 0.4 Ma (Burger et al., 1997; Boy et al., 2012; von Seckendorff, 2012; Voigt et al., 2022).

The described eryopid material from the Remigiusberg quarry comes from the lower Theisbergstegen lake level (sensu Boy et al., 2012) and is here referred to the base of the middle part of the Remigiusberg Formation (Fig. 2). One of the eryopid specimens (holotype; Fig. 2) was preserved in a dark grayish unbedded carbonaceous mudstone (unit 3; Fig. 2) with abundant intraformational pebbles interpreted to represent mudflow deposition in a shallow subaquatic lacustrine paleoenvironment. The other described eryopid specimen (paratype; Fig. 2) was preserved in greenish phytoturbated massive mudstone (unit 4; Fig. 2) of a supposed lake shoreline paleoenvironment. More detailed information on the litho- and biofacies of the Remigiusberg Formation at the Remigiusberg quarry are given in Voigt et al. (2019, p. 229–232).

Materials and methods

This work is based on two eryopid specimens discovered at the southwest German Remigiusberg quarry near Kusel, Rhineland–Palatinate, in autumn 2013 (paratype) and spring 2018 (holotype). Both specimens are represented by disarticulated bone material consisting of the skull with remains of the mandibles (holotype) and an incomplete skull, mandibles, and anterior postcranial material (paratype), respectively. The remains seem to be derived from partially to largely fully decomposed skeletons that were transported into a marginal lacustrine paleoenvironment. The holotype specimen is closely associated with non-eryopid, probably microsaur bone remains.

Preparation of the specimens was carried out mechanically by one of us (LR) and Georg Sommer from the Naturhistorisches Museum Schloss Bertholdsburg Schleusingen (NHMS). Photographs were taken with a Nikon D5100. Drawings were prepared from an A3-photograph and with a 'camera lucida' at a Motic binocular.

The new eryopid specimens are stored at the Urweltmuseum GEOSKOP/Lichtenberg Castle near Kusel (UGKU) but are owned by the state of Rhineland–Palatinate according to the local heritage protection law and, thus, inventory numbers refer to the Natural History Museum Mainz/State Collection of Natural History of Rhineland–Palatinate (NHMMZ/LS).

Repositories and institutional abbreviations.—CM, Carnegie Museum of Natural History, Pittsburgh, Pennsylvania; CMNH, Cleveland Museum of Natural History, Cleveland, Ohio; FMNH, Field Museum of Natural History, Chicago, Illinois; MCZ, Museum of Comparative Zoology of the Harvard University, Cambridge, Massachusetts; MHNA, Museum of Natural History, Autun, France; MMG, Museum für Mineralogie und Geologie, Dresden, Germany; NHMMZ/LS, Natural History Museum Mainz/State Collection of Natural History of Rhineland–Palatinate, Germany; NHMS, Naturhistorisches Museum Schloss Bertholdsburg, Schleusingen, Germany; NMMNH, New Mexico Museum of Natural History, Albuquerque, New Mexico; UGKU, Urweltmuseum GEOSKOP/Lichtenberg Castle near Kusel, Germany.

Systematic paleontology

Tetrapoda Jaekel, 1909
Amphibia Linneaus, 1758
Temnospondyli von Zittel, 1888
Eryopidae Cope, 1882

https://doi.org/10.1017/jpa.2023.58 Published online by Cambridge University Press

Diagnosis.—Synapomorphies (after Sawin, 1941; Romer, 1947; Milner, 1989, 1990; Boy, 1990; Werneburg and Steyer, 1999; Schoch and Hampe, 2004; Werneburg, 2007; Werneburg and Berman, 2012; Schoch and Milner, 2014): (1) enlarged choana medially wide; (2) ectopterygoid, palatine and vomer only with two or three fangs (without subsequent smaller teeth); (3) lacrimal reaches anteriorly to the naris or septomaxilla; (4) enlarged posterior width of skull (pS_w/S_l = 0.92–1.10); (5) posterior part of the cultriform process widened (partly); (6) interclavicle of adults proportionally small and broadly ovate in outline; (7) ilium with vertically directed dorsal process, which is anteroposteriorly widened dorsally.

Stenokranio new genus

Types species.—*Stenokranio boldi* n. gen. n. sp.

Diagnosis.—As for type species by monotypy.

Etymology.—Greek στενός (stenos) for narrow, κρανίο (kranio) for skull.

Remarks.—None.

Stenokranio boldi new species
Figures 3–11, 12.1–12.3, 13–15, 17, 18.1, 19.1

Holotype.—NHMMZ/LS PW 2019/5025 (formerly: UGKU 2564), consisting of the skull with skull roof and palate, together with remains of the mandibles (skull length [elsewhere = midline skull length] 24.7 cm).

Paratype.—NHMMZ/LS PW 2019/5022 (formerly: UGKU 1998), consisting of the greater portion of skull roof, parts of the palate with palatine, choana and several pairs of fangs, and the mandible in lateral view (skull length 27 cm), together with a few bones of the anterior postcranium.

Diagnosis.—Autapomorphies: (1) small posterior skull width (pS_w/S_l = 0.92) and posterior half of skull with nearly longitudinally straight margins; (2) postparietals and tabulars forming a longitudinally short bony strip; (3) ectopterygoid very wide, its most posterior part and neighboring pterygoid equal in width.

Synapomorphies with some of the eryopids.—(1) Density of sculpture pattern quantified as the number of pits per in^2 on frontal + jugal in relation to skull length range between 0.64 and 1.42, and bones of normal thickness, in contrast to the thinner bones in *Glaukerpeton* Romer, 1952; (2) small width of skull table between lateral margins of supratemporals (H_w/S_l = 0.42–0.43), in contrast to *Glaukerpeton* and *Actinodon* Gaudry, 1866; (3) equal internarial and interorbital width, in contrast to *Glaukerpeton*, in which the internarial width is smaller; (4) occipital margin of skull roof is relatively straight and only slightly concave, only shared with *Onchiodon thuringiensis*; (5) septomaxilla is completely sculptured, shared with *Onchiodon* Geinitz, 1862, and in contrast to *Eryops* and *Glaukerpeton* with a smooth anterior portion of the bone; (6) no interfrontal, in contrast to *Eryops*; (7) no lateral line sulci, in contrast to *Glaukerpeton* and *Actinodon*; (8) palatine is very wide, only shared with *Glaukerpeton*; (9) fang pair of ectopterygoid and vomer of equal size (in contrast to *Onchiodon*, in which ectopterygoid fangs are smaller), and consist of two teeth (in contrast to *Glaukerpeton* with three ectopterygoid teeth); (10) straight dorsal margin of the surangular process and the participation of the posterior half of coronoid 3 in this process with the same height; surangular process is relatively low in comparison to the maximum height of the mandible, in contrast to the second eryopid from Remigiusberg; (11) dentary with approximately 48–50 marginal tooth positions, in contrast to the lower number in the second eryopid from Remigiusberg; (12) homodont marginal dentition of mandible and maxilla, with the size of the teeth generally small and gradually decreasing from rostral to abrostral; parasymphyseal teeth are similar in size to the adjacent dentary teeth; this stands in contrast to the second eryopid from Remigiusberg, *Eryops*, and *Onchiodon* with a rather heterodont dentition of larger teeth; (13) low coracoid region, angle between supraglenoid buttress and anterior margin of scapular blade is 90° or slightly greater, in contrast to *Glaukerpeton* and *Onchiodon labyrinthicus* Geinitz, 1862.

Occurrence.—Remigiusberg quarry at the northeastern rim of the Remigiusberg (387685 E, 5487644 N, UTM 32U, WGS 84; UGKU L-21), ~1 km northeast of Haschbach, Kusel County, western Rhineland–Palatinate, Germany (Voigt et al., 2014, 2019; Fig. 1). Type horizon is a mudstone of the lower Theisbergstegen lake level, middle part of the Remigiusberg Formation, base of Rotliegend, Gzhelian–Asselian boundary, latest Carboniferous or earliest Permian (Figs. 1, 2).

Comparative description.—The two specimens are similar in size with skull lengths of 24.7 cm (holotype) and 27 cm (paratype), respectively. Their possession of shared characters such as the very similar skull roof proportions (Table 1), posteriorly notched orbits, and the similar type of dermal sculpturing indicate that they belong to the same taxon.

General skull morphology.—The dermal sculpture of the dorsal skull roof corresponds to the relatively coarse sculpture pattern known from most eryopids (Werneburg and Berman, 2012; Table 2). The dermal sculpture of the dorsal skull roof consists of a reticulated pattern of small pits and valleys separated by narrow ridges (Figs. 3, 9.1, 9.2). The nasal shows much more radially directed ridges on the smaller holotypic skull roof (Fig. 3) than on the larger paratypic skull with a close reticulate system (Fig. 9.1). The density of the sculpture pattern is quantified as the number of pits per in^2 (6.452 cm^2) on the frontal and jugal, which are typically well-preserved bones in eryopid skulls, and as a proportion of those counts to skull length. These intraspecific indices range between elements and specimens of *Stenokranio* n. gen. between 0.64 and 1.42, which are very similar in *Onchiodon* and *Eryops* specimens. The dermal sculpture of the dorsal skull roof in similar-sized *Glaukerpeton* specimens is of much finer sculpture pattern with indices from 2.6 to 4.0 (Werneburg and Berman, 2012).

Most eryopid skulls exhibit a dorsal strutting pattern with large ridges, as in *Eryops* and *Onchiodon*, which increased the mechanical stability of the skull (Sawin, 1941; Boy, 1990; Werneburg, 2007). A paired, well-developed and large

https://doi.org/10.1017/jpa.2023.58 Published online by Cambridge University Press

Figure 3. *Stenokranio boldi* n. gen. n. sp., skull roof in dorsal view, holotype NHMMZ/LS PW 2019/5025, with the anterior view of the right premaxilla; note the low and nearly equal height of the teeth.

longitudinal ridge extends from the lateral portion of the tabular and supratemporal to the postorbital. The ridge then runs on the post- and prefrontal and the median part of the nasal to the premaxilla, where it forms a median wall to the naris (Fig. 17.1). This pair of longitudinal ridges is consistent in both skulls. Additional transverse ridges may occur between the longitudinal ridges on parietals, frontals, and nasals. These transverse ridges are differently pronounced and most completely developed on the paratype skull roof (Fig. 10.1). Depressions are present between these ridges. Also, the ridges on the jugal are variable. A Y-shaped ridge is developed on the anterior part of the jugal in the holotypic skull, whereas a curved ridge extending from the prefrontal is present on the anterior part of the jugal in the paratypic skull.

The degree of skull roof ossification is relatively high, and the bones are normally thick as in other eryopids, but in contrast to the 30–50% thinner skull roof bones of *Glaukerpeton*.

https://doi.org/10.1017/jpa.2023.58 Published online by Cambridge University Press

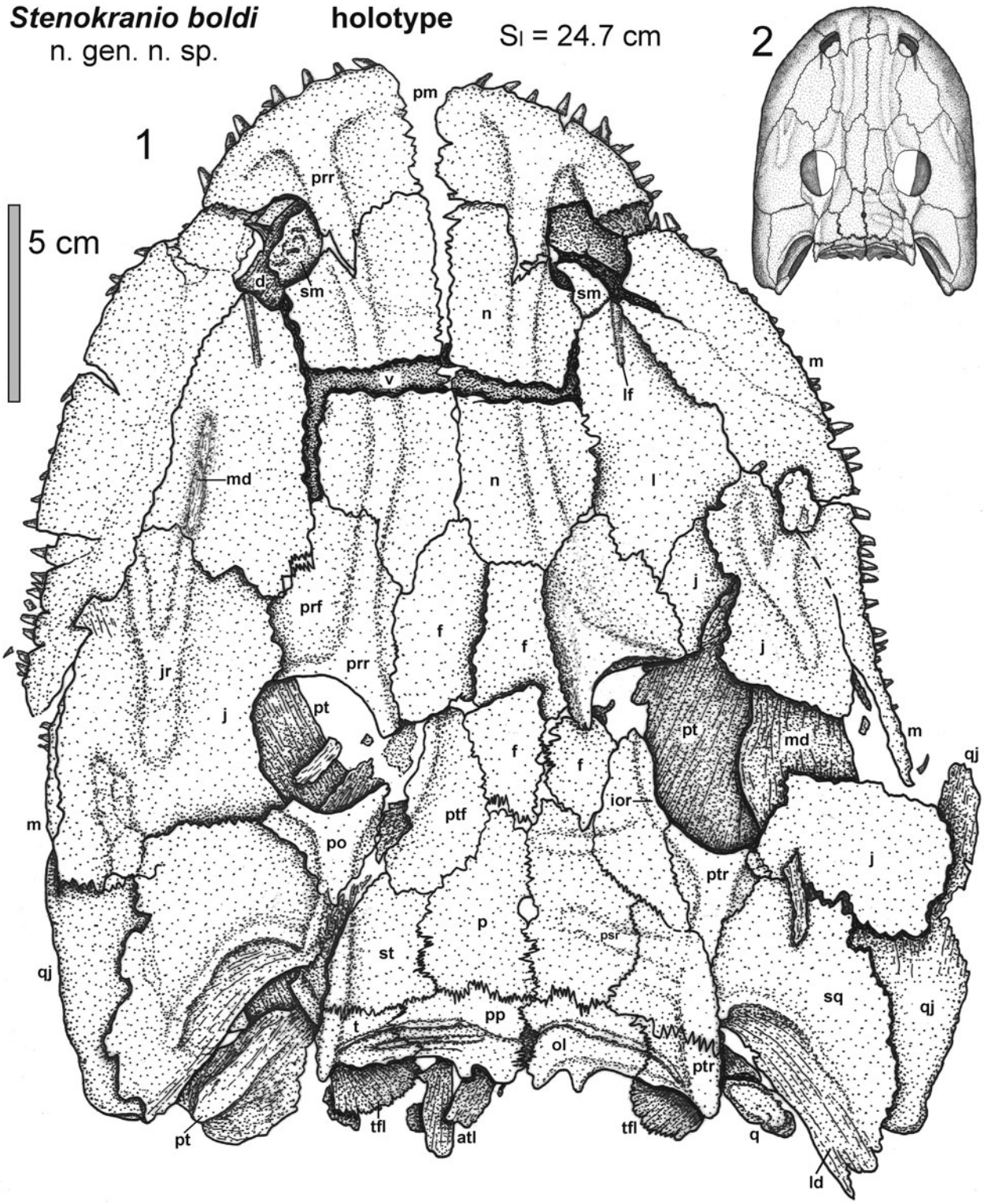

Figure 4. *Stenokranio boldi* n. gen. n. sp., skull roof in dorsal view, holotype NHMMZ/LS PW 2019/5025. (**1**) Interpretative drawing with atlas; (**2**) reconstruction. atl = atlas; d = dentary; f = frontal; ior = intraorbital ridge; j = jugal; jr = jugal ridge; l = lacrimal; ld = lamina descendens; lf = lacrimal furrow; m = maxilla; md = mandible; n = nasal; ol = occipital lamella; p = parietal; pm = premaxilla; po = postorbital; pp = postparietal; prf = prefrontal; prr = prefrontal-rostral ridge; psr = parietal-supratemporal ridge; pt = pterygoid; ptf = postfrontal; ptr = postorbital-tabular ridge; q = quadrate; qj = quadratojugal; S_l = skull length; sm = septomaxilla; sq = squamosal; st = supratemporal; t = tabular; tfl = tabular flange; v = vomer.

The combination of both known skulls of *Stenokranio* n. gen. allowed a tentative reconstruction of the skull roof in dorsal view and of the palate in ventral view (Fig. 17.1, 17.2). The skull is longer than wide. In dorsal view the lateral margin of the skull describes a wide parabolic curve with a broad, bluntly rounded snout and a short postorbital region. The

https://doi.org/10.1017/jpa.2023.58 Published online by Cambridge University Press

Figure 5. *Stenokranio boldi* n. gen. n. sp., holotype, NHMMZ/LS PW 2019/5025. (**1**) Palate in ventral view, with both mandibles, atlas, and external tetrapod bones (see Fig. 15); (**2**) teeth between pterygoid and vomer; (**3**) tooth-like palatal denticles on vomer; (**4**) left stapes (in the lower right part of the image) with stapedial foramen.

width of the posterior skull is unusually small in comparison with other eryopids ($pS_w/S_l = 0.92$; see Table 1). Therefore, *Stenokranio* n. gen. has a skull with nearly parallel lateral margins, which is a unique character in eryopids. The postorbital width of the skull measured between the lateral margins of the supratemporals is small ($H_w/S_l = 0.42–0.43$) in contrast to that of *Glaukerpeton* and *Actinodon*. The preorbital skull is elongate ($PO_l/S_l = 0.60–0.61$), similar to large skulls of *Eryops* or

https://doi.org/10.1017/jpa.2023.58 Published online by Cambridge University Press

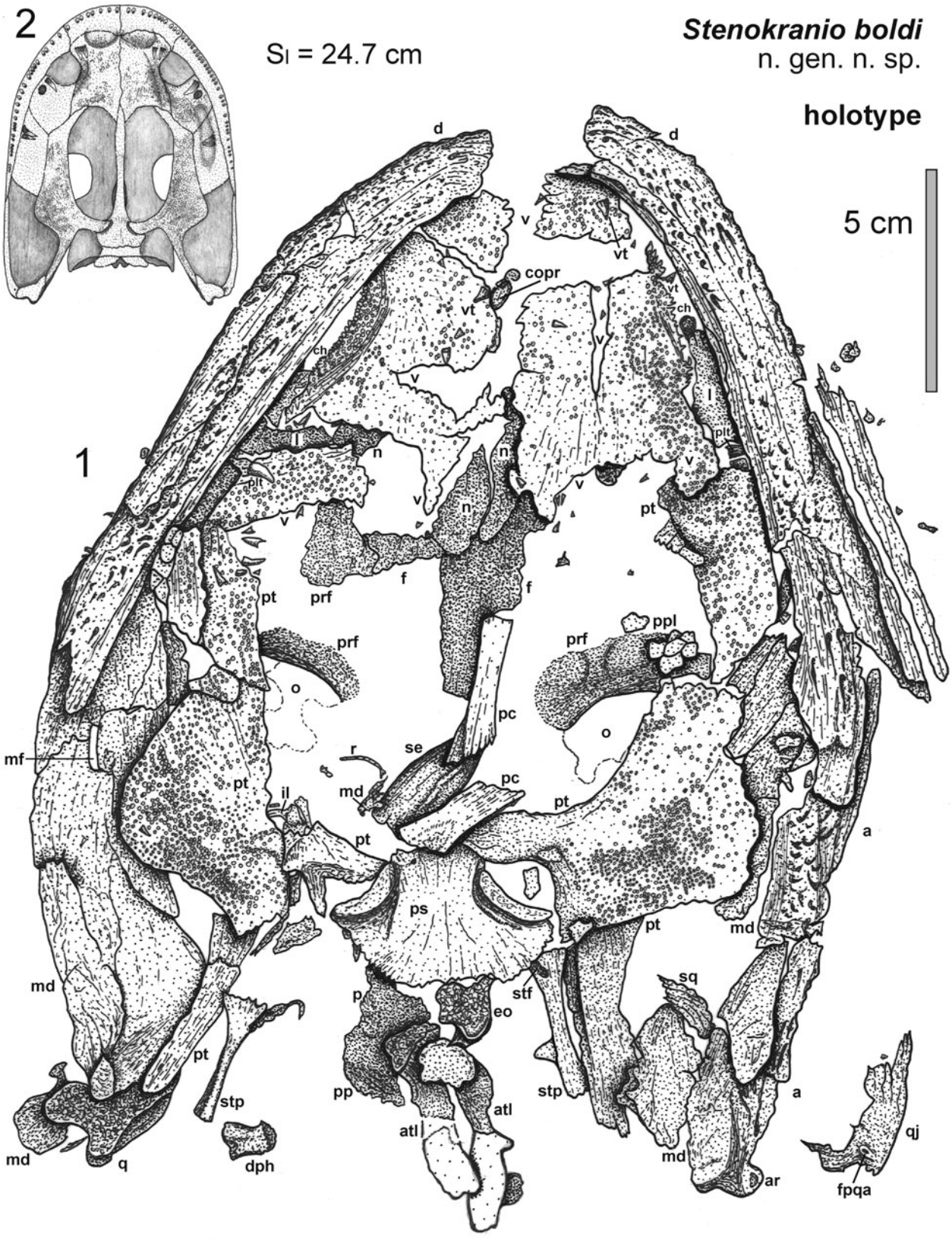

Figure 6. *Stenokranio boldi* n. gen. n. sp., palate in ventral view, with both mandibles, atlas, and external tetrapod bones (see Fig. 15), holotype NHMMZ/LS PW 2019/5025. (**1**) Interpretative drawing; (**2**) reconstruction. a = angular; ar = articular; atl = atlas; ch = choane; copr = coprolith; d = dentary; dph = diadectid phalangal; eo = exoccipital; f = frontal; fpqa = quadratojugal foramen accessory; il = ilium; l = lacrimal; md = mandible; mf = meckelian fenestra; n = nasal; o = orbit; p = parietal; pc = cultriform process of parasphenoid; plt = palatine tooth; pp = postparietal; ppl = palatal plates; prf = prefrontal; ps = parasphenoid; pt = pterygoid; q = quadrate; qj = quadratojugal; r = rib; se = sphenethmoid; S_l = skull length; sq = squamosal; stf = stapedial foramen; stp = stapes; v = vomer; vt = vomerine tooth.

https://doi.org/10.1017/jpa.2023.58 Published online by Cambridge University Press

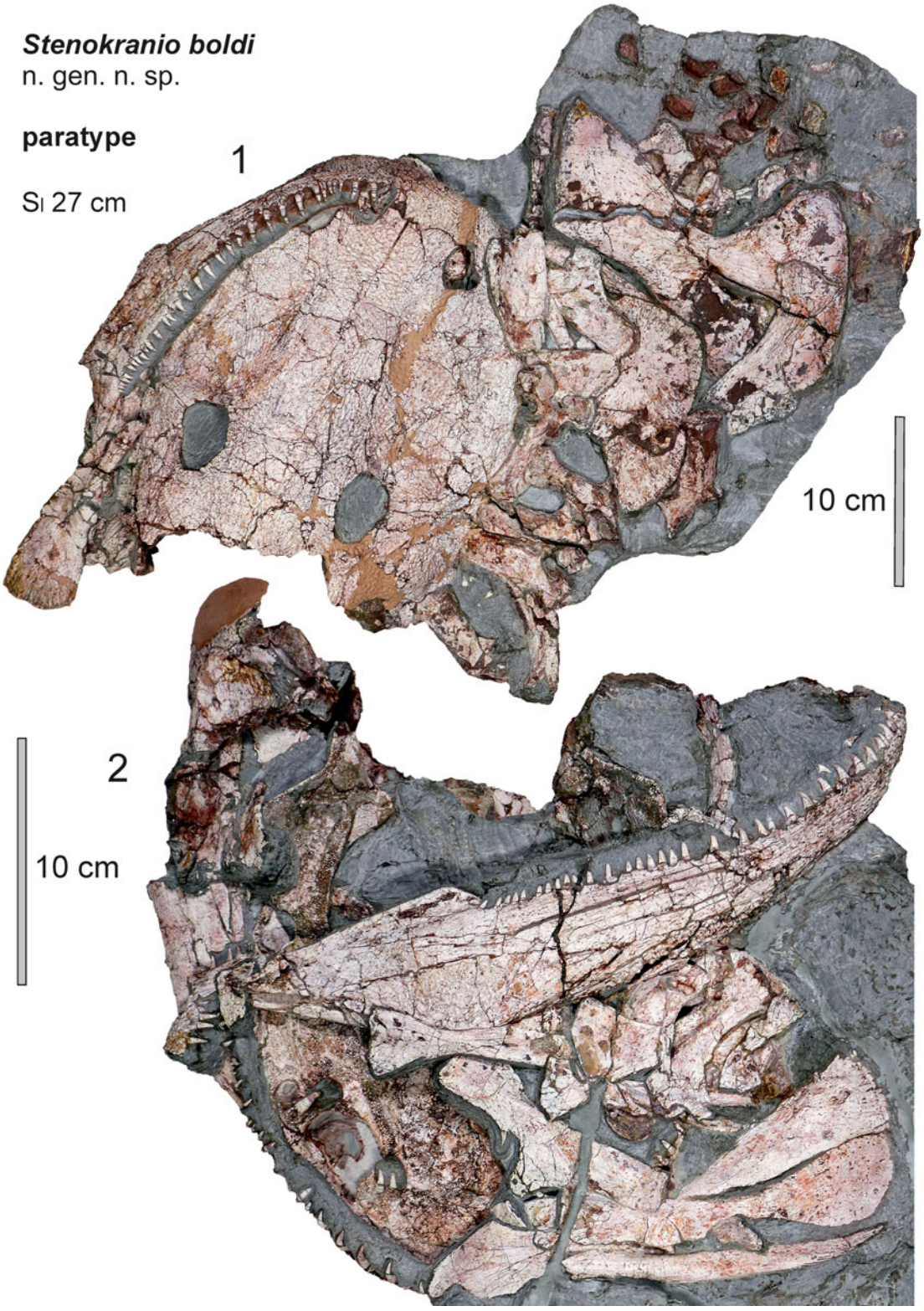

Figure 7. *Stenokranio boldi* n. gen. n. sp., skull with mandibles and anterior postcranial skeleton, paratype NHMMZ/LS PW 2019/5022. (**1**) Dorsal skull roof with left mandible, shoulder girdle, and anterior axial skeleton; (**2**) palatal skull in ventral view, right mandible in labial view, shoulder girdle, and ribs. S_l = skull length.

Onchiodon thuringiensis. The internarial and interorbital width are equal ($IN_w/S_l = IO_w/S_l = 0.24$ in the holotype and = 0.26/0.27 in the paratype), as in most eryopids, but in contrast both to *Glaukerpeton*, in which the internarial width is smaller, and to *Eryops megacephalus* Cope, 1878, with a smaller interorbital width (Table 1). The occipital margin of the skull roof is

https://doi.org/10.1017/jpa.2023.58 Published online by Cambridge University Press

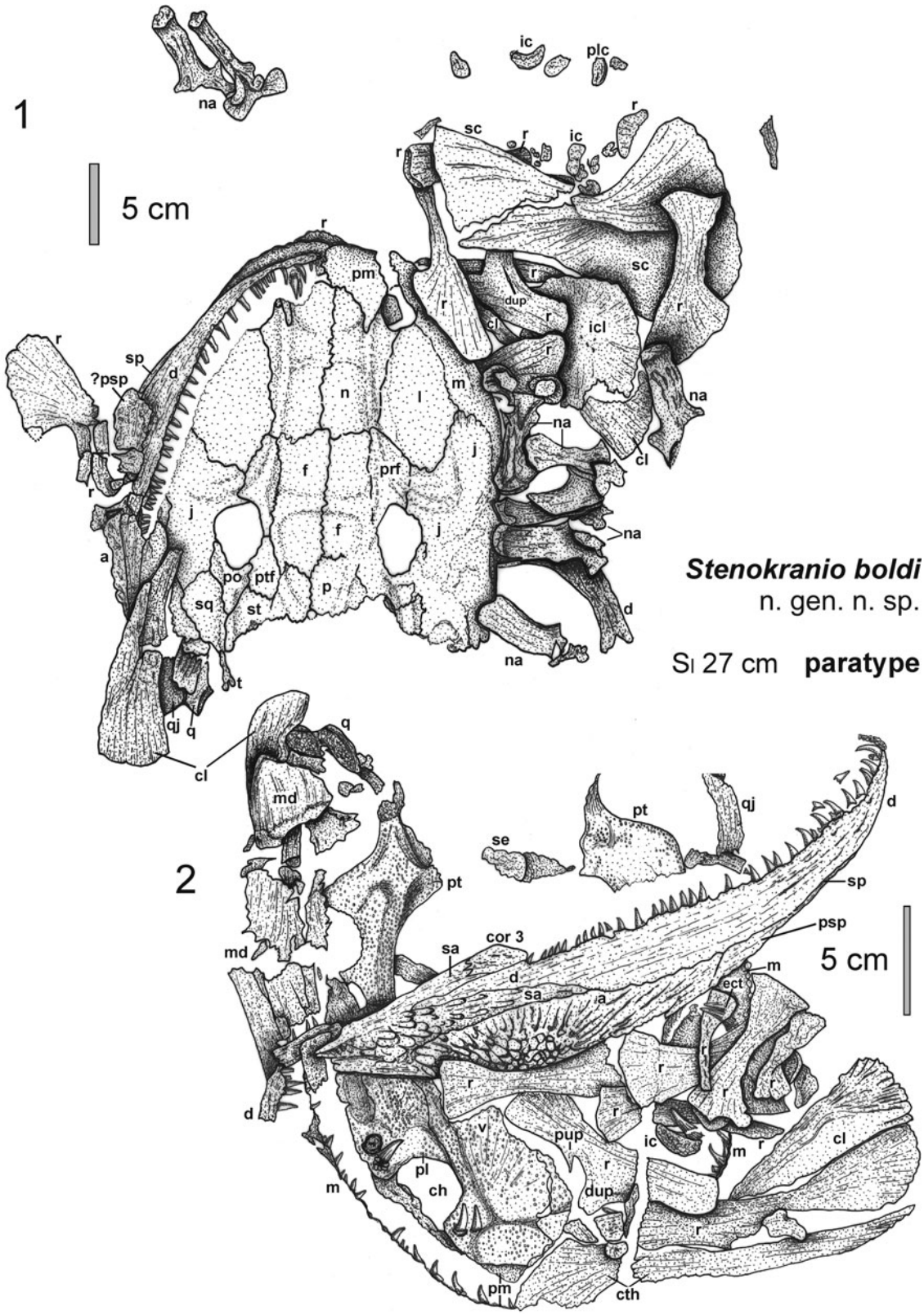

Figure 8. *Stenokranio boldi* n. gen. n. sp., interpretative drawing of skull with mandibles and anterior postcranial skeleton, paratype NHMMZ/LS PW 2019/5022. (**1**) Dorsal skull roof with left mandible, shoulder girdle, and anterior axial skeleton; (**2**) palatal skull in ventral view, right mandible in labial view, shoulder girdle, and ribs. a = angular; ch = choane; cl = clavicle; cor 3 = coronoid 3; cth = cleithrum; d = dentary; dup = distal uncinate process; ect = ectopterygoid teeth; f = frontal; ic = intercentrum; icl = interclavicle; j = jugal; l = lacrimal; m = maxilla; md = mandible; n = nasal; na = neural arch; p = parietal; pl = palatine; plc = pleurocentrum; pm = premaxilla; po = postorbital; prf = prefrontal; psp = postsplenial; pt = pterygoid; ptf = postfrontal; pup = proximal uncinate process; q = quadrate; qj = quadratojugal; r = rib; sa = surangular; sc = scapulocoracoid; se = sphenethmoid; S_l = skull length; sp = splenial; sq = squamosal; st = supratemporal; t = tabular; v = vomer.

https://doi.org/10.1017/jpa.2023.58 Published online by Cambridge University Press

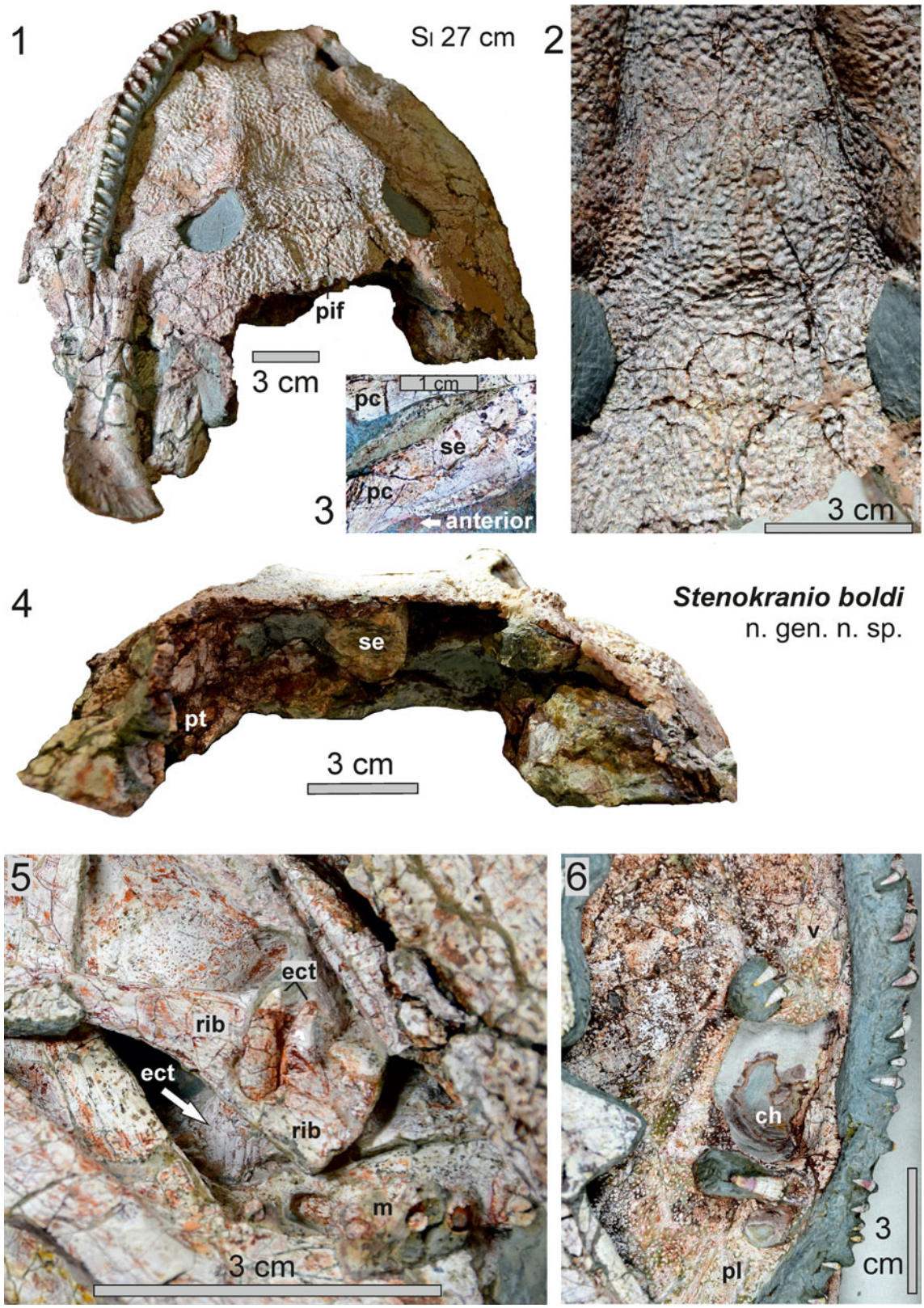

Figure 9. *Stenokranio boldi* n. gen. n. sp., skull in various views, paratype NHMMZ/LS PW 2019/5022. (**1**) Skull roof in posterodorsal view, with left mandible and left clavicle; note the dorsal strutting pattern with large longitudinal ridges; (**2**) dermal sculpture of the dorsomedian skull roof; (**3**) sphenethmoid with longitudinal, ventral ridge (holotype NHMMZ/LS PW 2019/5025); (**4**) skull in posterior view, note the nearly uncompacted natural skull shape, and the compact sphenethmoid below the pineal foramen; (**5**) large ectopterygoid fang pair pierce the first or second rib without fracture; (**6**) wide choana and palatine with large fang, and vomer with fang pair and intensive denticulation as well as teeth of premaxilla and maxilla. ch = choane; ect = ectopterygoid teeth; m = maxilla; pc = cultriform process; pif = pineal foramen; pl = palatine; pt = pterygoid; rib = rib; se = sphenethmoid; S_l = skull length; v = vomer.

https://doi.org/10.1017/jpa.2023.58 Published online by Cambridge University Press

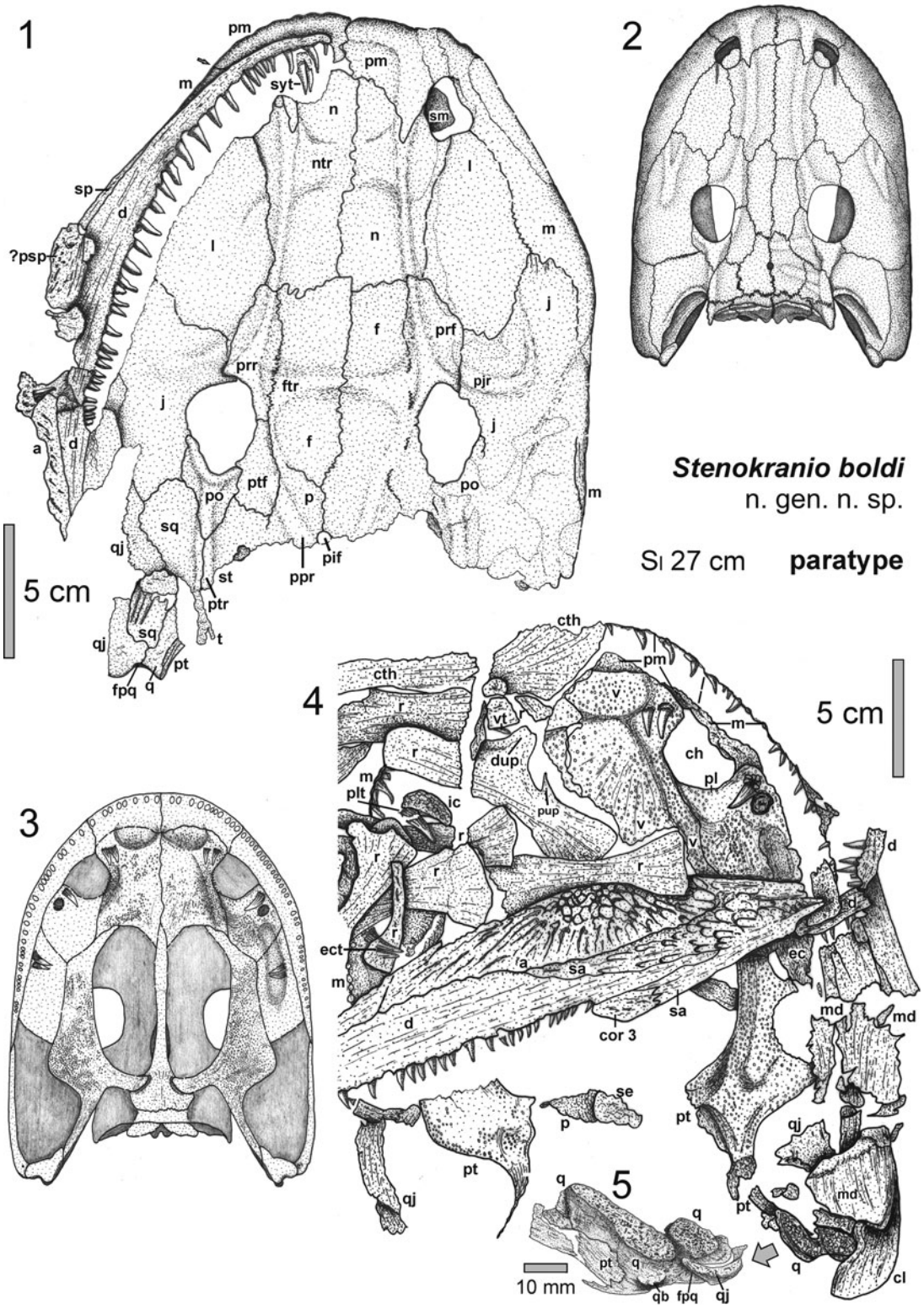

Figure 10. *Stenokranio boldi* n. gen. n. sp., interpretative drawing of skull with mandibles and anterior postcranial skeleton, paratype NHMMZ/LS PW 2019/5022. (**1**) Dorsal skull roof with left mandible; the arrow indicates the suture between premaxilla and maxilla; (**2**) reconstruction of dorsal skull roof; (**3**) reconstruction of ventral palatal skull; (**4**) palatal skull in ventral view, with, ribs, intercentrum, and cleithrum; (**5**) enlarged quadrate condyle in ventral view. a = angular; ch = choane; cl = clavicle; cor 3 = coronoid 3; cth = cleithrum; d = dentary; dup = distal uncinate process; ec = ectopterygoid; ect = ectopterygoid teeth; f = frontal; fpq = quadratojugal foramen; ftr = frontal transverse ridge; ic = intercentrum; j = jugal; l = lacrimal; m = maxilla; md = mandible; n = nasal; ntr = nasal transverse ridge; p = parietal; pif = pineal foramen; pjr = prefrontal–jugal ridge; pl = palatine; plt = palatine tooth; pm = premaxilla; po = postorbital; ppr = postfrontal-parietal ridge; prf = prefrontal; prr = prefrontal-rostral ridge; psp = postsplenial; pt = pterygoid; ptf = postfrontal; ptr = postorbital–tabular ridge; pup = proximal uncinate process; q = quadrate; qb = quadrate boss; qj = quadratojugal; r = rib; sa = surangular; se = sphenethmoid; S_l = skull length; sm = septomaxilla; sp = splenial; sq = squamosal; st = supratemporal; syt = symphyseal teeth; t = tabular; v = vomer; vt = vomerine tooth.

https://doi.org/10.1017/jpa.2023.58 Published online by Cambridge University Press

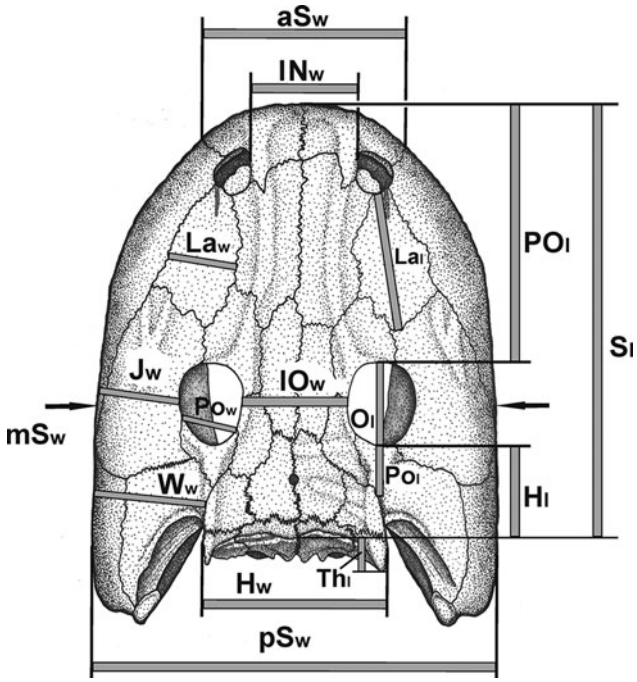

Figure 11. Measured distances of the reconstructed skull roof from *Stenokranio boldi* n. gen. n. sp. aS_w = anterior width of skull at level of maxilla-premaxilla sutures; H_l = postorbital midline length of skull from level of posterior margins of orbits; H_w = postorbital width of skull between lateral margins of supratemporals; IN_w = minimum internarial width; IO_w = minimum interorbital width; J_w = transverse width of jugal at maximum lateral lacrimal extent of orbit; La_l = maximum length of lacrimal; La_w = maximum transverse width of lacrimal; mS_w = midlength width of skull at midlength level of orbits; O_l = maximum length of orbit; PO_l = preorbital midline length of skull from level of anterior margins of orbits; Po_l = maximum posterior length of postorbital from posteriormost extent of orbit; Po_w = maximum transverse width of postorbital at contribution to orbital margin; pS_w = maximum posterior width of skull at level of posterolateral margins of cheeks; S_l = midline skull length; Th_l = length of tabular horn region between levels of posterior tabular corner and occipital midline margin; W_w = maximum transverse width of cheek from lateral margin of supratemporal anterior to otic notch.

relatively straight and only slightly concave, as in *O. thuringiensis*. The quadrate condyles lie distinctly posterior to the occipital condyles. The orbits are large compared to most other eryopids (O_l/S_l = 0.17–0.19). They bear a posterior notch formed by the postorbital.

Growth stage.—Both known specimens of *Stenokranio* n. gen. are clearly adult animals because (1) the dermal sculpture consists of a reticulated pattern of small pits and valleys separated by narrow ridges; (2) exoccipitals, sphenethmoid (partly) and quadrate are well ossified; (3) vertebrae have ossified inter- and pleurocentra, neural arches with well-developed transverse processes and high spinous processes; (4) ribs present large uncinate processes; (5) scapulocoracoid is well ossified; (6) the skull length of 24–27 cm is large in the family Eryopidae and only *Eryops*, *O. thuringiensis*, and *Osteophorus* (Meyer, 1860a) have larger skulls. However, two characters of the *Stenokranio* n. gen. specimens indicate that they are early adult, and they did not reach the late adult or senile stage: (1) sphenethmoid is very narrow and probably only partly ossified, and (2) basioccipital is not ossified.

Skull roof (Figs. 4, 7.1, 8.1, 9.1, 9.2, 10.1, 17.1, 18).—The interpremaxillary suture is elongated and accounts for ~13% of the midline length of the skull. This is similar to *Glaukerpeton* and *Eryops megacephalus*, whereas this suture is proportionally shorter in the Pennsylvanian *Eryops* of New Mexico (Werneburg et al., 2010). The alary process of the premaxilla is relatively wide as in *Onchiodon labyrinthicus* (Boy, 1990) but stronger in the Pennsylvanian *Eryops*. The premaxilla has 14 tooth loci in its ventral tooth arcade.

The rounded oval- to triangular-shaped naris is elongated, as in *Glaukerpeton* or *Eryops megacephalus*, comprising 11% of the midline length of the skull. The kidney-shaped septomaxilla is completely sculptured (Fig. 4.1) and is completely located in a dorsal position at the posteromedial part of the naris (shared with *Onchiodon*). It covered about one-third of the area of the narial opening and excludes the nasal from the naris. The mostly ventrally directed and smooth septomaxilla in *Eryops* occupies almost the entire naris proper (Sawin, 1941).

The lacrimal is roughly diamond shaped. It is separated from the orbit by an elongated contact between jugal and prefrontal. However, the anterior part of the lacrimal is wide, as in *Glaukerpeton* or *Eryops megacephalus*, and participates in the posterolateral narial margin. A short, narrow, anterior–posteriorly directed furrow is visible in this part of the bone and is interpreted as the ductus nasolacrimalis (holotypic skull in Figs. 3, 4.1). It is completely closed in the slightly larger paratypic skull (Figs. 7.1, 10.1). This duct is closed earlier in the late juvenile stage of *O. labyrinthicus* (Boy, 1990, fig. 2). A groove for the lacrimal duct is also known from the lacrimal in *Eryops* (Sawin, 1941, p. 419). The maxilla has a wide dorsal shelf, especially near the lacrimal–jugal suture and about 40 tooth loci in its ventral tooth arcade. The nasal is considerably elongated and narrow as is typical of eryopids with the exception of *O. thuringiensis* in which the nasal is anterolaterally wider. The frontal is narrow as in most other eryopids.

The jugal is proportionally wider than in *Glaukerpeton* or *Actinodon* but proportionally narrower than in *O. thuringiensis*. The postorbital is triangular in outline and has an angled (or notched) orbital margin. The postfrontal and prefrontal clearly contact one another as in all eryopids, but their dorsal orbital processes are proportionally much wider than in *Glaukerpeton* and *Actinodon*. The prefrontal is anteriorly widened and the postfrontal is posteriorly elongated and wide. Together with the shortened postorbital skull table this leads to the shortening of the supratemporal, which is approximately as long as wide and is one of the proportionally shortest supratemporals in eryopids. Only in *Clamorosaurus borealis* Gubin, 1983, is the supratemporal much wider than long (RW and FW in preparation).

The parietals extend anterior to the posterior orbital margin. Posteriorly, they nearly reach a common transverse line with the posterior margin of the short supratemporals, which is a unique situation in eryopids. The parietal foramen lies at the transversal line at the posterior end of postfrontals (Figs. 3, 4, 9.2) and is not located in a smooth depression on the parietals as described in *O. thuringiensis*. *Stenokranio* n. gen. bears the shortest postparietals and tabulars in eryopids. These bones form a continuous short strip at the slightly concave occipital margin, as in *O. thuringiensis*. The tabular horn is short (Th_l/S_l = 0.06). The occipital lamella is medially bilobed and anteriorly bordered by one or two transverse ridges (Fig. 4.1). The tabular bears a pronounced ventrally directed tabular flange. In accordance

https://doi.org/10.1017/jpa.2023.58 Published online by Cambridge University Press

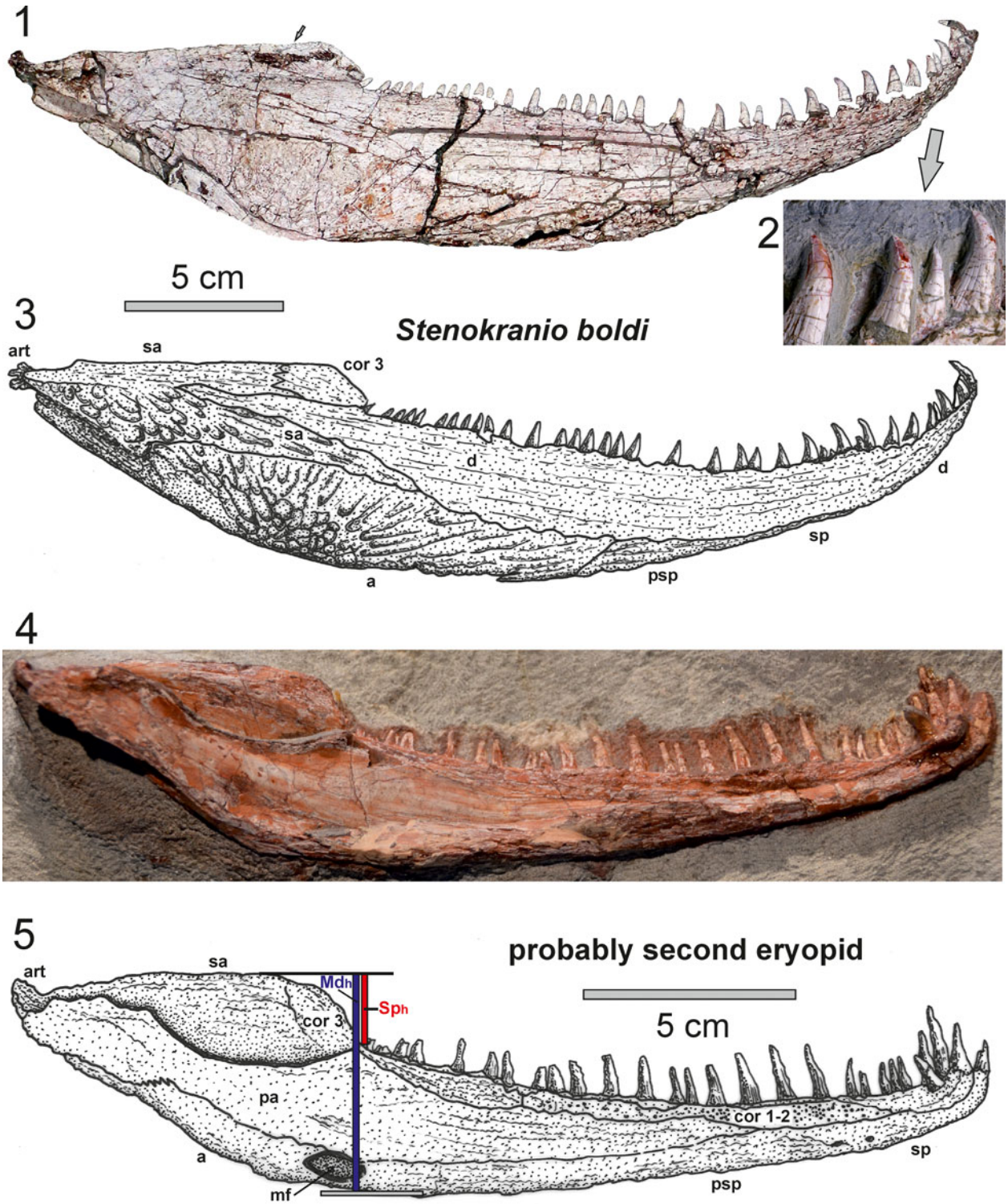

Figure 12. Two different eryopid mandibles from the Remigiusberg quarry. (**1–3**) Right mandible of *Stenokranio boldi* n. gen. n. sp., in labial view, note the sharp carina on the anterior teeth (**2**), length 232 mm, paratype NHMMZ/LS PW 2019/5022;the small arrow indicates the suture between surangular and coronoid 3; (**4, 5**) left mandible of a probable eryopid in lingual view, length 213 mm, NHMMZ/LS PW 2019/5020 (former: POL-F 2012-001), after Witzmann (2013). a = angular; art = articular; cor 3 = coronoid 3; d = dentary; mf = meckelian fenestra; pa = prearticular; psp = postsplenial; sa = surangular; sp = splenial; Md_h = mandibular height; Sp_h = surangular height.

with the generally slender cheek ($W_w/S_l = 0.26$), the squamosal and quadratojugal are relatively narrow. In *Onchiodon* and *Actinodon* the cheek is proportionally wider whereas *Glaukerpeton* has the proportionally narrowest cheeks (Table 1).

In *Stenokranio* n. gen. the exposure of the quadrate on the occipital surface of the cheek (Figs. 4.1, 10.1) consists of a narrow, dorsally short process that is directed anteromedially between the squamosal and the quadrate ramus of the pterygoid.

https://doi.org/10.1017/jpa.2023.58 Published online by Cambridge University Press

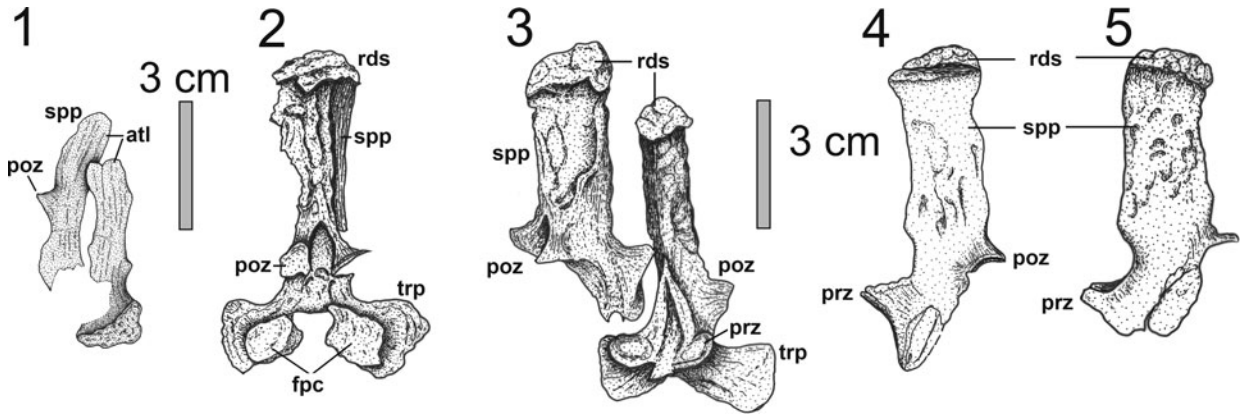

Figure 13. *Stenokranio boldi* n. gen. n. sp., interpretative drawing of neural arches. (**1**) Atlas in lateral view, holotype NHMMZ/LS PW 2019/5025; (**2**) anteriormost neural arch in posterolateral view; (**3**) two neural arches in lateral and anterolateral view; (**4, 5**) neural arches in lateral view, (**2–5**) paratype NHMMZ/LS PW 2019/5022. atl = atlas; fpc = facets for pleurocentra; poz = postzygapophysis; prz = prezygapophysis; rds = roughened dorsal surface; spp = spinose process; trp = transversal process.

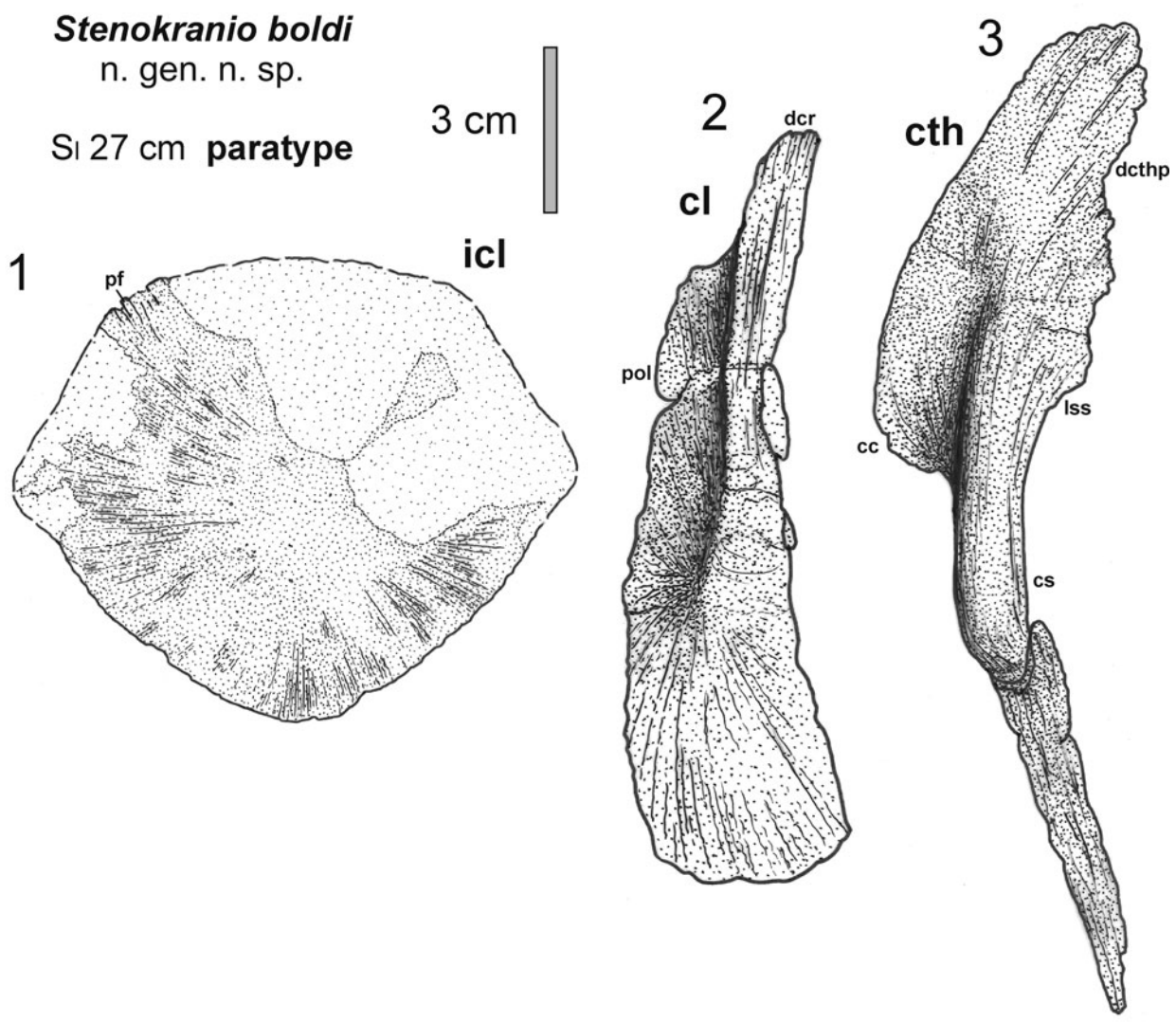

Figure 14. *Stenokranio boldi* n. gen. n. sp., interpretative drawing of shoulder girdle bones, paratype NHMMZ/LS PW 2019/5022. (**1**) Interclavicle in dorsal view; (**2**) left clavicle in dorsal view; (**3**) left cleithrum in lateral view. cc = cleithral crest; cl = clavicle; cs = cleithral shaft; cth = cleithrum; dcr = dorsal clavicular rod; dcthp = dorsal cleithral process; icl = interclavicle; lss = suprascapular lamina; pf = pectinate fringe; pol = posterior lamina of clavicle.

https://doi.org/10.1017/jpa.2023.58 Published online by Cambridge University Press

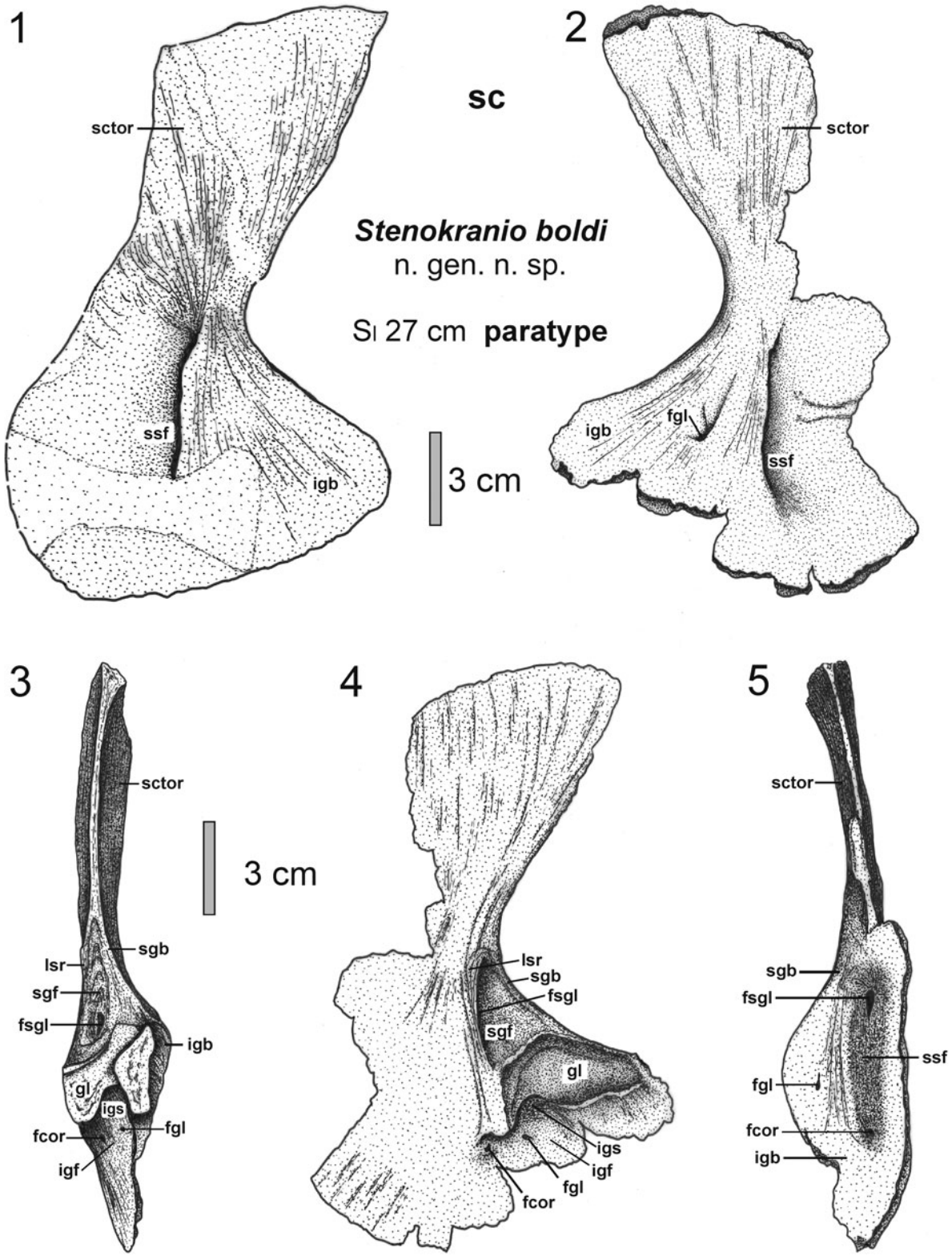

Figure 15. *Stenokranio boldi* n. gen. n. sp., interpretative drawing of both scapulocoracoids, paratype NHMMZ/LS PW 2019/5022. (**1**) Right scapulocoracoid from medial view; (**2–5**) left scapulocoracoid (**2**) in medial view, (**3**) in posterior view, (**4**) in lateral view, (**5**) in anterior view. fcor = coracoid foramen; fgl = glenoid foramen; fsgl = supraglenoid foramen; gl = glenoid fossa; igb = intraglenoid buttress; igf = infraglenoid fossa; igs = infraglenoid recess; lsr = lateral supraglenoid ridge; sc = scapulocoracoid; sctor = scapular torus (scapular blade); sgb = supraglenoid buttress; sgf = supraglenoid fossa; S_l = midline skull length; ssf = subscapular fossa.

https://doi.org/10.1017/jpa.2023.58 Published online by Cambridge University Press

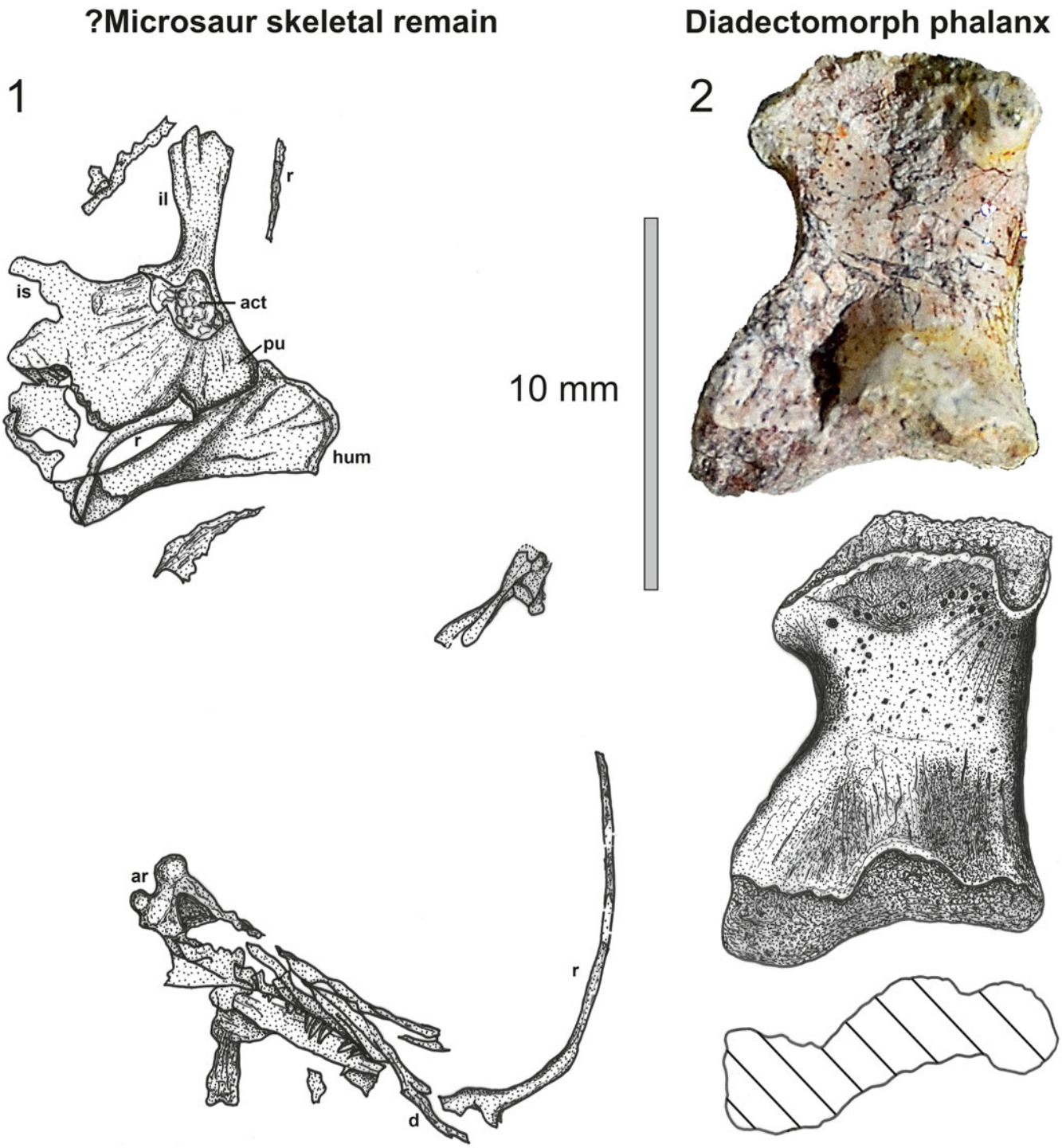

Figure 16. Foreign tetrapod bones from the palatal skull of *Stenokranio boldi* n. gen. n. sp. (compare Figs. 5 and 6.1), holotype NHMMZ/LS PW 2019/5025. (**1**) Interpretative drawing of a possible microsaur skeletal remains with the pelvis in lateral view, ribs, ?humerus, and mandible; (**2**) photo and interpretative drawing of a diadectomorph phalanx, with cross section (diagonal-line fill). act = acetabulum; ar = articular; d = dentary; hum = humerus; il = ilium; is = ischium; pu = pubis; r = rib.

In *Eryops* and *Glaukerpeton* this construction is very similar, but the dorsal portion of the quadrate is anteromedially more elongated whereas in *O. thuringiensis* it is similarly short but wider. A transverse strip-like dorsal part of the quadrate is known in *O. labyrinthicus* and *Actinodon* (Fig. 18). A well-developed, boss-like protuberance occurs at the ventral margin of the dorsal quadrate process in *Stenokranio* n. gen., *Glaukerpeton*, and *O. labyrinthicus*. In *Stenokranio* n. gen., *Onchiodon*, and *Eryops* a quadratojugal foramen near the posterolateral margin of the quadratojugal is visible only in ventral view of the skull (Figs. 6.1, 10.1). In *Glaukerpeton*, the foramen is visible in lateral and dorsal views of the skull roof. In the *Eryops* sp. specimen

https://doi.org/10.1017/jpa.2023.58 Published online by Cambridge University Press

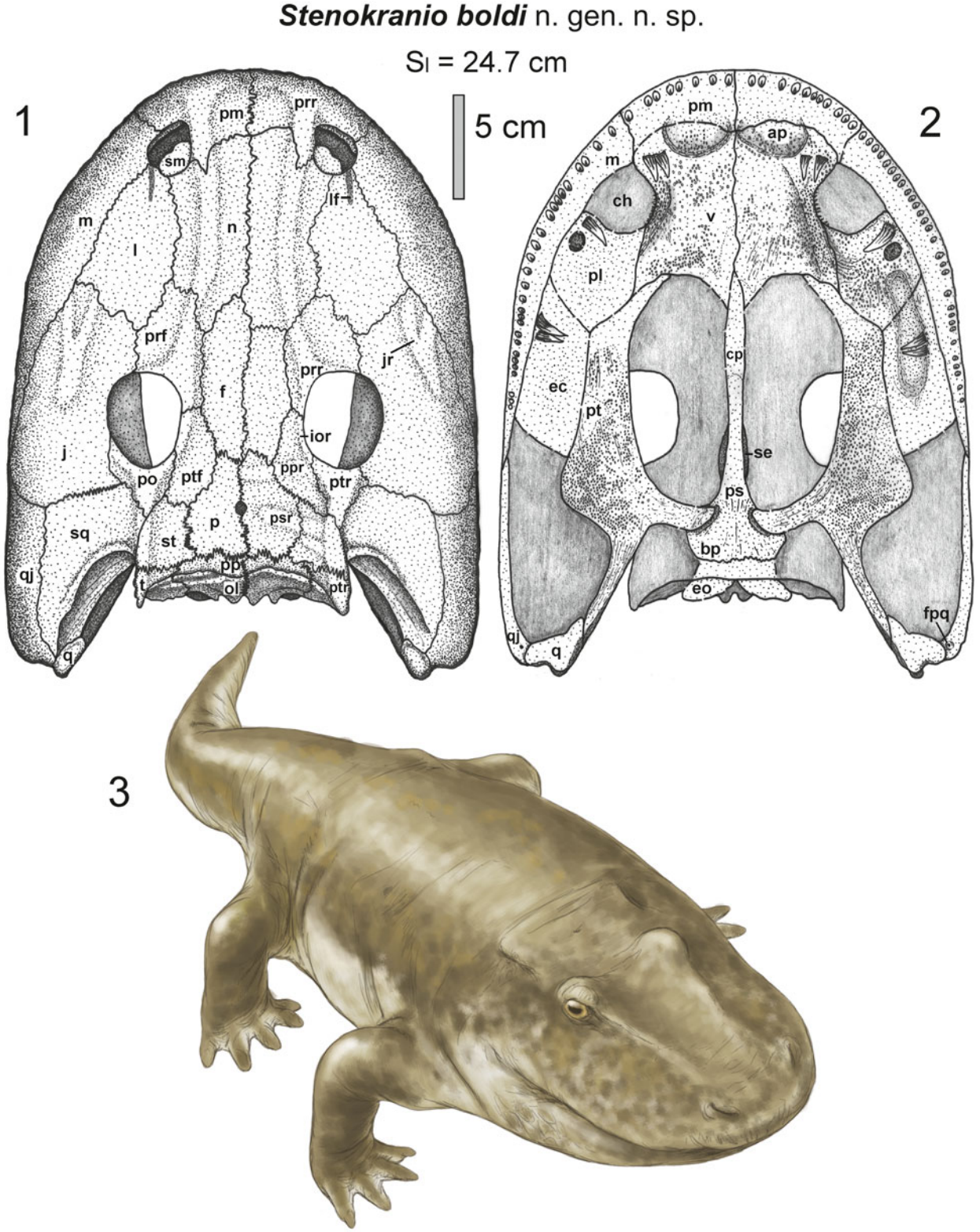

Figure 17. *Stenokranio boldi* n. gen. n. sp., reconstruction of the new eryopid. (**1**) Dorsal skull roof; (**2**) palatal skull; (**3**) life restoration of the whole animal (artwork by Frederik Spindler, Kipfenberg). ap = anterior palatal depression; bp = basal plate of parasphenoid; ch = choane; cp = cultriform process; ec = ectopterygoid; eo = exoccipital; f = frontal; fpq = quadratojugal foramen; ior = intraorbital ridge; j = jugal; jr = jugal ridge; l = lacrimal; lf = lacrimal furrow; m = maxilla; n = nasal; ol = occipital lamella; p = parietal; pl = palatine; pm = premaxilla; po = postorbital; pp = postparietal; ppr = postfrontal-parietal ridge; prf = prefrontal; prr = prefrontal-rostral ridge; ps = parasphenoid; psr = parietal-supratemporal ridge; pt = pterygoid; ptf = postfrontal; ptr = postorbital-tabular ridge; q = quadrate; qj = quadratojugal; se = sphenethmoid; S_l = midline skull length; sm = septomaxilla; sq = squamosal; st = supratemporal; t = tabular; v = vomer.

https://doi.org/10.1017/jpa.2023.58 Published online by Cambridge University Press

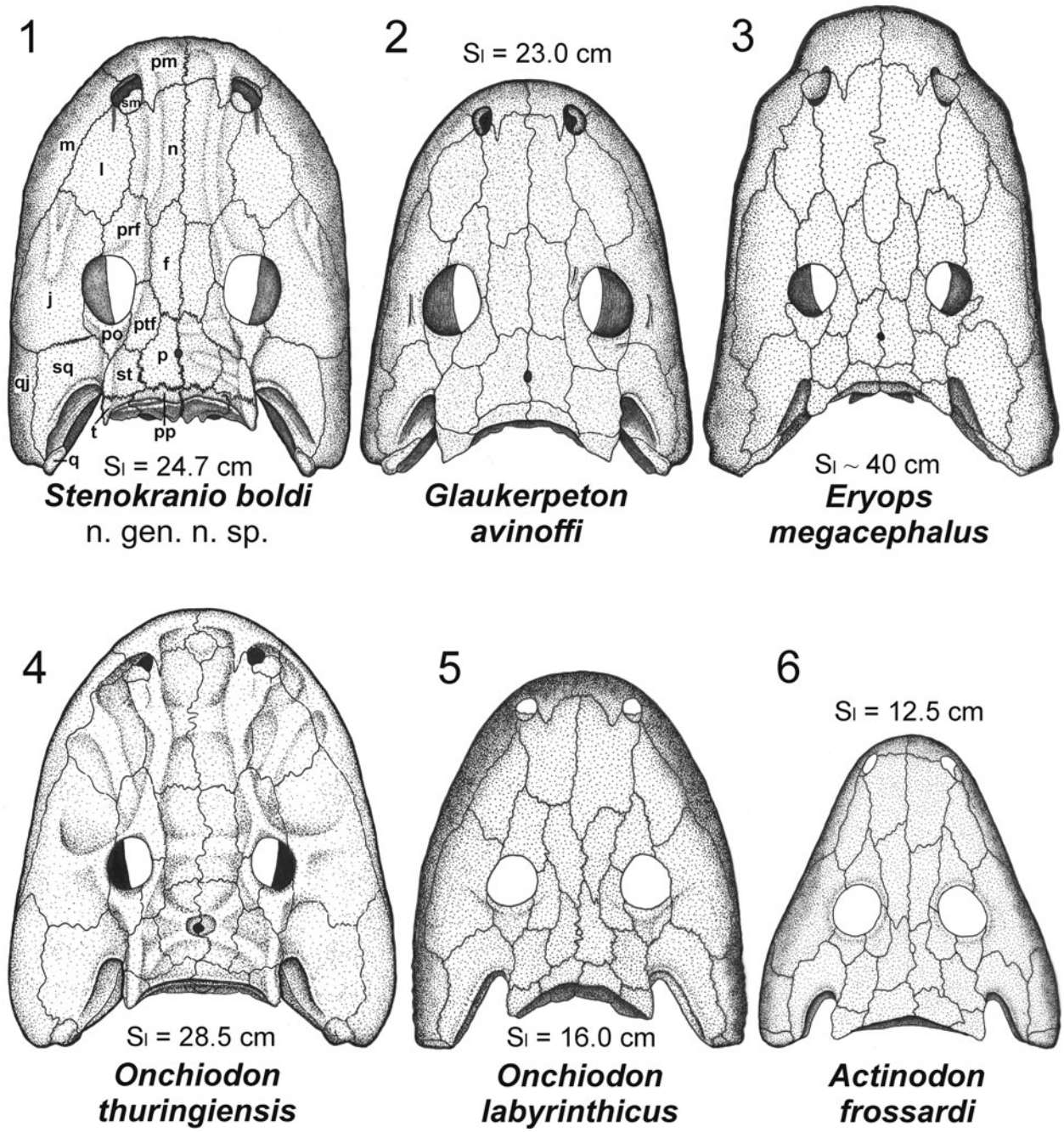

Figure 18. Comparison of eryopid skull roofs in dorsal view. (**1**) *Stenokranio boldi* n. gen. n. sp., from this paper. (**2**) *Glaukerpeton avinoffi*, after Werneburg and Berman (2012). (**3**) *Eryops megacephalus*, after Sawin (1941). (**4**) *Onchiodon thuringiensis*, after Werneburg (2007). (**5**) *Onchiodon labyrinthicus*, after Boy (1991). (**6**) *Actinodon frossardi*, after Werneburg (1997). f = frontal; j = jugal; l = lacrimal; m = maxilla; n = nasal; p = parietal; pm = premaxilla; po = postorbital; pp = postparietal; prf = prefrontal; ptf = postfrontal; q = quadrate; qj = quadratojugal; S_I = midline skull length; sm = septomaxilla; sq = squamosal; st = supratemporal; t = tabular.

NMMNH P-46379 from the Late Pennsylvanian of New Mexico two small and one larger quadratojugal foramen are visible at the posteroventral margin of the quadratojugal only in dorsal and lateral views of the skull roof (Werneburg et al., 2010).

Lateral line sulci are not present in *Stenokranio* n. gen. and only known among postlarval forms of *Glaukerpeton* and *Actinodon* (Werneburg, 1997; Werneburg and Berman, 2012). However, Warren (2007) argued that at least an enclosed quadratojugal lateral line canal is present in *Eryops*.

Palate and braincase (Figs. 5–8, 9.3–9.5, 10.3, 10.4, 17.2, 19).—In addition to the skull roof, the palate is informationally complete in both skulls. The pattern of thickened longitudinal ridges on the palatal bones is only partly preserved. A pronounced, narrow ridge starts posterior to the vomerine tusks and borders the choana medially (Figs. 5, 6, 9.5, 10.4, 19.1). Another elevated longitudinal structure starts posterior to the palatine fang pair and continues posteriorly on more than half the length of the ectopterygoid (Figs. 9.5, 10.4, 19.1), as in *O. thuringiensis*.

https://doi.org/10.1017/jpa.2023.58 Published online by Cambridge University Press

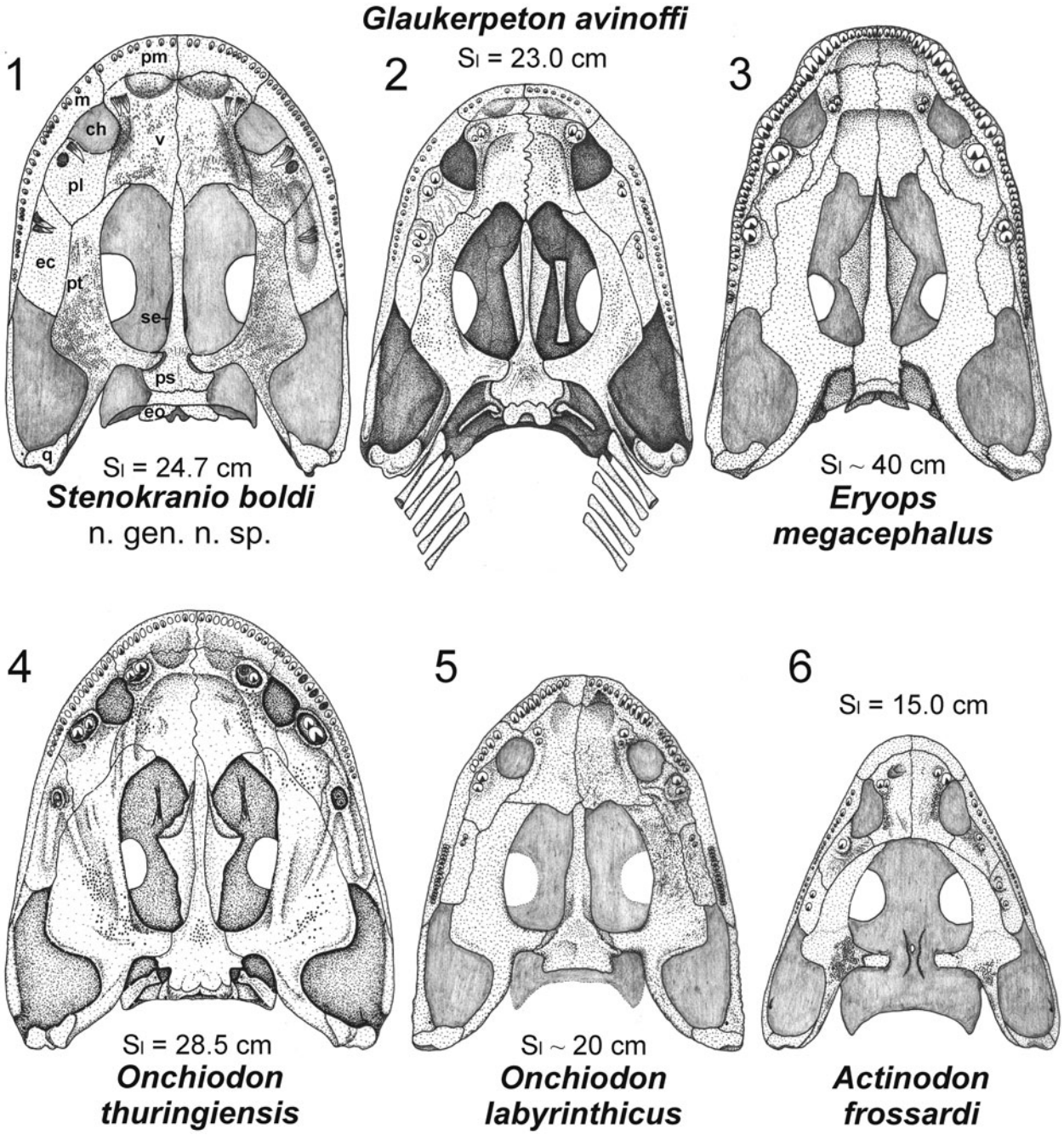

Figure 19. Comparison of eryopid skulls in palatal view. (**1**) *Stenokranio boldi* n. gen. n. sp., from this paper (**2**) *Glaukerpeton avinoffi*, after Werneburg and Berman (2012). (**3**) *Eryops megacephalus*, after Sawin (1941). (**4**) *Onchiodon thuringiensis*, after Werneburg (2007). (**5**) *Onchiodon labyrinthicus*, after Boy (1991). (**6**) *Actinodon frossardi*, after Werneburg and Steyer (1999). ch = choane; ec = ectopterygoid; eo = exoccipital; m = maxilla; pl = palatine; pm = premaxilla; ps = parasphenoid; pt = pterygoid; q = quadrate; se = sphenethmoid; v = vomer.

Just anterior to the transverse level of the vomerine tusks, the anterior palatal fossae extend mostly on the anterior part of the vomers (Fig. 10.4) and probably on the dental shelf of the premaxilla. The anterior palatal fossae are restricted to the premaxillae in *Glaukerpeton* because these bones extend posteriorly almost to the level of the vomerine tusks.

The vomer is elongated and wide. The smallest width of both vomers (= interchoanal width) is clearly wider than the interorbital width in *Stenokranio* n. gen., *Eryops*, and *Onchiodon*. In contrast, the interchoanal and interorbital width is equal in *Glaukerpeton* and *Actinodon*. The process-like posterolateral corner of the vomer in *Stenokranio* n. gen., *Glaukerpeton*, and *Onchiodon* extends a short distance between the pterygoid and palatine (Figs. 6.1, 10.4), although it is much narrower in the latter, whereas in the Permian and Pennsylvanian *Eryops* the process is much longer and vermiform. The suture between vomer and palatine is much more elongated than in *Glaukerpeton* and *Actinodon*. The palatine is short and very wide and only *Glaukerpeton* has a similarly shaped palatine. The ectopterygoid is unusually wide (Fig. 10.4, and by

https://doi.org/10.1017/jpa.2023.58 Published online by Cambridge University Press

Table 1. Comparative measurements of adult eryopid skulls (important values in bold; after Boy, 1990; Werneburg, 1997, 2007; Werneburg and Berman, 2012).

	Stenokranio boldi n. gen. n. sp.		*Glaukerpeton avinoffi*	*Eryops* sp.	*Eryops megacephalus*	*Onchiodon thuringiensis*	*Onchiodon labyrinthicus*	*Actinodon frossardi*	
	NHMMZ/LS PW 2019/5025	NHMMZ/LS PW 2019/5022	CM 8539, CMNH 11025	MCZ 1914	MCZ 1129, holotype	NHMS-WP 2140a	Boy (1990, Abb. 2F)	MHNA 15/10/62	MMG FrP1
S_l in mm	247	270	230	320	364	285	160	111	123
pS_w/S_l	**0.92**	—	**0.99**	0.94	0.94	**1.06**	**1.07**	**1.10**	**1.09**
mS_w/S_l	0.91	0.85	0.89	0.94	0.83	0.97	1.00	0.90	0.88
aS_w/S_l	0.47	0.52	0.49–0.50	0.47	0.49	0.48	0.50	**0.38**	**0.38**
H_w/S_l	**0.42**	**0.43**	**0.56**	0.44	0.38	0.43	0.47	**0.53**	**0.54**
H_l/S_l	0.22	0.23	0.25–0.26	0.22	0.17	0.24	0.25	**0.27**	**0.28**
PO_l/S_l	**0.60**	**0.61**	**0.55**	0.63	0.68	0.62	0.58	0.54	0.53
IN_w/S_l	**0.24**	**0.26**	**0.21**	0.26	0.26	0.26	0.26	0.20	0.23
IO_w/S_l	**0.24**	**0.27**	**0.29**	0.28	0.23	0.27	0.26	**0.20**	**0.21**
O_l/S_l	0.19	0.17	0.20–0.21	0.15	0.14	0.15	0.18	0.18	0.19
La_w/La_l	0.54	0.51	0.35–0.49	0.30	0.40	0.62	0.35	0.37	0.35
Po_w/Po_l	~1.0	0.83	0.83–1.05	1.06	1.20	0.80	1.23	1.33	0.89
Ju_w/S_l	0.16	0.16	0.11	**0.23**	0.14	**0.20**	0.17	0.16	0.15
W_w/S_l	0.26	—	0.20–0.22	0.28	0.26	0.31	0.32	0.29	0.28
Th_l/S_l	0.06	—	0.12	0.07	0.09	0.08	0.10	0.10	0.08

reconstruction in Fig. 19.1) in contrast to all other eryopids. Its posteriormost part is equal in width to the neighboring pterygoid. The dentition of all three palatal bones consists of one pair of fangs on each bone (Figs. 6.1, 9.4, 9.5, 10.4). The fang pair of the palatine is the largest, and the fang pairs of the vomer and ectopterygoid slightly smaller and of equal size. *Glaukerpeton* has three fangs and both species of *Onchiodon* present one pair of very small teeth on the ectopterygoid.

The choana is shortened and nearly circular (Fig. 9.5). This character of *Stenokranio* n. gen. is in contrast to that of *Glaukerpeton*, *Actinodon*, and *Eryops* in which the choanae are more elongate. The anterior margin of the choana exhibits a short, narrow, V-shaped notch of variable development lateral to the alveolus of the vomerine tusks as in all eryopids except for *O. labyrinthicus*.

The pterygoid (Figs. 5, 6, 10.4) has a narrow palatinal ramus as in *Glaukerpeton*, *Eryops*, and *Actinodon*. The anterior third of the the palatinal branch forms a sharp anteromedially directed corner, similar to *Eryops* and *O. labyrinthicus*. The transverse flange of the pterygoid in *Stenokranio* n. gen., *Glaukerpeton*, and *Eryops* exhibits a low, angular expansion. In *Onchiodon* and *Actinodon*, on the other hand, the entire, free, lateral margin of the pterygoid is greatly expanded into a right-angled projection. The interpterygoid vacuities were filled with mosaics of irregular polygonal bony plates without preserved denticles (Fig. 6).

In *Stenokranio* n. gen., *Glaukerpeton*, and *Onchiodon* the basicranial union is formed by the basipterygoid process of the pterygoid suturally overlapping the ventral surface of the anterolateral corner of the parasphenoidal basal plate (Fig. 6). In *Eryops*, in contrast, a short, stout, laterally projecting basipterygoid process of the braincase unites with the internal process of the pterygoid in a nearly vertical interdigitating suture. The cultriform process of the parasphenoid is generally narrow (Fig. 6), has a broad triangular base, and it is narrower at midlength. Anteriorly, it becomes a little wider again and abruptly narrows at its distal end in accordance with the posteromedial vomers and it extends a short distance between the midline union of the vomers. The cultriform process in *O. labyrinthicus* and *Eryops* is swollen in its posterior half with convex lateral margins. The cultriform process supports a diamond-outlined sphenethmoid in *Eryops*, *Glaukerpeton*, and *O. thuringiensis*. However, the sphenethmoid is much less ossified in *Stenokranio* n. gen. It is only slightly wider than the cultriform process and bears a longitudinal, ventral ridge (Fig. 6, 9.3). The sphenethmoid is triangular in cross section and massive (Fig. 9.4). The ventral surface of the parasphenoidal basal plate is smooth and lacks a denticle field, but a fine groove for the carotid artery closely parallels the medial margin of the facet for the internal process of the pterygoid (Fig. 6). The basal plate is wide in contrast to *Eryops* and short as in *O. labyrinthicus*. The basioccipital probably was not ossified in this growth stage of *Stenokranio* n. gen., whereas the separate exoccipitals are well ossified.

Table 2. Ranges of density counts of dermal sculpture pits and valleys of frontal and jugal in relation to the skull length (in cm) given separately and combined for eryopids and grouped by genus, species, and maturity (partly after Werneburg and Berman, 2012); p = number of dermal skull pits or valleys per in^2 (= 6.452 cm^2), mainly from frontal and jugal at midlength level of orbits.

Eryopid groups	frontal-p/S_l	jugal-p/S_l	range of p/S_l
Stenokranio boldi n. gen. n. sp. from the Pennsylvanian–Permian boundary (Germany)	0.72–1.42	0.64–1.13	0.64–1.42
Late Pennsylvanian *Glaukerpeton* (Pennsylvania, West Virginia)	2.6–3.3	3.2–4.0	2.6–4.0
Pennsylvanian *Eryops* (El Cobre Canyon, New Mexico)	1.3	1.7	1.3–1.7
Early Permian *Eryops grandis* (New Mexico and Utah)	0.5–1.6	1.1	0.5–1.6
Adult Permian *Eryops*	0.4–1.1 1.8	0.5–1.0	0.4–1.1
subadult Permian *Eryops*	6.8–12.0	1.2–4.3	1.2–4.3
Juvenile *Eryops* (all Early Permian of Texas)		—	6.8–12.0
Early Permian *Onchiodon thuringiensis* (Germany)	1.0	—	1.0

https://doi.org/10.1017/jpa.2023.58 Published online by Cambridge University Press

Numerous denticles are present on the whole vomer, on the palatinal branch of the pterygoid, partly on the palatine, and probably on the ectopterygoid. Some of the denticles on the pterygoid and vomer are of equal size to the posteriormost maxillary teeth (Fig. 6). The parasphenoid is free of denticulation.

The articular condyle of the quadrate is transversely expanded and divided into a pair of condylar facets (Figs. 6.1, 10.5). A narrow, notch-like channel that separates the quadrate condyle from the posterior end of the ventral margin of the quadratojugal is absent in *Stenokranio* n. gen., *Eryops*, *O. labyrinthicus*, and *Actinodon*, but established in *Glaukerpeton* and *O. thuringiensis*.

Visceral skeleton.—The only preserved elements of the visceral skeleton are the stapes (Fig. 6). The footplates are widened and pierced by the stapedial foramen. The shaft is elongated as in *Eryops* (Sawin, 1941, pl. 6), keel-like thin in ventral/dorsal view, and 1.5–2.0 times wider and flattened in posterior/anterior view. The shaft of the stapes in *O. thuringiensis* is wider and probably shorter (Werneburg, 2007, fig. 8b).

Mandibles (Figs. 5–8, 9.1, 10.1, 10.4, 12.1–12.3).—The mandibles of *Stenokranio* n. gen. are mostly preserved in labial aspect. In the holotypic skull the posterior mandibular bones are badly preserved in lingual view, but the low, oval meckelian fenestra is well established (Figs. 5, 6). The right mandible is completely preserved in labial view (Figs. 7.2, 8.2, 12.1–12.3). It exhibits a morphology that, with few exceptions, is very similar to that of *Glaukerpeton* and *Eryops*. One of these shared characters is the straight dorsal margin of the surangular process and the participation of the posterior half of coronoid 3 in that process with the same height. The dorsal surangular process is relatively low in comparison with the maximum height of the mandible (the height of the step of the dorsal surangular process above the level of the most posterior tooth arcade in relation to the mandibular height at this point is 0.23). The mandibles indicate 48–50 marginal tooth positions (Figs. 8.2, 10.1). The marginal teeth of the mandible are small compared to those of the maxilla, and in contrast to the development of a caniniform region in *Eryops*. All tips of the dentary teeth form a relatively straight line. The pair of parasymphyseal teeth and the marginal teeth on the dentary are of equal size (Fig. 10.1).

Dentition resembles that of other aquatic temnospondyl relatives with a basal labyrinthodont infolding of enamel and dentine resulting in distinct longitudinal grooves. All the marginal teeth are curved lingually (Fig. 12.1–12.3), but the fangs are directed posteriorly. The upper, smooth part of the teeth show mesiodistally aligned, well-developed carinae (Fig. 12.2).

An isolated 21-cm-long mandible (POL-F 2012-001), also found at the locus typicus Remigiusberg quarry of the new eryopid described here, was reported by Witzmann (2013) as the stratigraphically oldest eryopoid of the Saar–Nahe basin and tentatively assigned to eryopids. This mandible presents its lingual side (Fig. 12.4, 12.5), whereas the new eryopid *Stenokranio* n. gen. shows a perfect labially preserved mandible of ~30 cm length (Fig. 12.1–12.3). One hypothesis is that this isolated mandible belongs to the new taxon, *Stenokranio* n. gen. However, some important differences of the eryopid mandible POL-F 2012-001 are (1) higher step of the dorsal surangular process (the height of the step of the dorsal surangular process above the level of the most posterior tooth arcade in relation to the mandibular height at this point is 0.33); (2) dorsal margin of coronoid 3 is not continuous with the straight dorsal margin of the surangular process; (3) only 35–40 marginal tooth positions; (4) generally longer teeth; (5) wave-like differentiation of mandibular teeth with two or three caniniform regions; and (6) meckelian fenestra is possibly dorsoventrally higher. Thus, the most parsimonious interpretation is that two eryopid taxa were present.

Postcranium (Figs. 7, 8, 10.4, 13–15).—Few bones of the anterior postcranial skeleton are associated with the 27-cm-long skull of the paratypic specimen. The paired neural arches of the atlas lie posterior to the 24.7-cm long holotypic skull. Additional vertebrae as well as ribs and the shoulder girdle are preserved.

The preserved axial elements of *Stenokranio* n. gen. are essentially identical to those in *Eryops* based on Moulton's (1974) detailed description of its vertebral column. The atlantal neural arch is narrow and has a relatively short, dorsally rounded spinous process above the triangular postzygapophyses (Fig. 13.1). The process-like ventral part of the atlas may belong to the centrum, which is similarly illustrated from the stereospondylomorph *Korkonterpeton* (Werneburg et al., 2020, fig. 10a, b). The preserved neural arches have spinous processes with rugose areas on the flanks (Fig. 13.2–13.5) and represent the most anterior vertebrae. The dorsal surface of the neural arches is roughened, similar to the basal stereospondylomorph *Sclerocephalus* (Boy, 1988; Schoch and Witzmann, 2009a). One pair of the transverse processes bear facets for the pleurocentra on their posterior faces. A few isolated pleuro- and intercentra are preserved but bear few details except for the fact that the intercentra are crescent-shaped as in *Eryops* (Figs. 8.1, 8.2, 10.4).

Numerous ribs are preserved, some of which are devoid of uncinate processes, whereas others bear one or two processes (distal and proximal). The natural position of these widened anterior ribs is well preserved in a skeleton of *Actinodon* from Autun in France (Werneburg, 1997, fig. 2). One rib of the paratype bears a special phenomenon (Fig. 9.4). Both teeth of the ectopterygoid fang pair pierce a rib without fracture. Thus, the bones of the tetrapod-Fossillagerstätte of the Remigiusberg must have passed through a plastic consistency during diagenesis of the sediments.

The shoulder girdle is well preserved in the paratype and includes the interclavicle, both clavicles, cleithra, and scapulocoracoids. Its morphology largely corresponds with that described in detail in *Eryops* by Pawley and Warren (2006).

The interclavicle is slightly wider than long, with pectinate fringes anteriorly (Fig. 14.1; $Icl_l/Icl_w = 0.82–0.90$). The posterolateral margins form a right angle with a more pointed posterior end. The interclavicle UGKU 3 of an *Eryops*-like temnospondyl from the Meisenheim Formation of Rockenhausen (Saar–Nahe Basin) differs from that of *Stenokranio* n. gen. in being much wider than long ($Icl_l/Icl_w = 0.70$; Witzmann and Voigt, 2014) and its posterior margin forming an obtuse angle. However, the shape of the interclavicle of *Stenokranio* n. gen. falls within the variability of the three different interclavicles of *Eryops* figured by Cope (1888, pl. 1, figs. 1, 2), Miner (1925, fig. 15), and Pawley and Warren (2006, fig. 3). The clavicula has a narrow ventral blade (Fig. 14.2). The cleithrum (Fig. 14.3), which is longer than the clavicle, has a massive shaft and a long-oval blade.

The right scapulocoracoid (Fig. 15.1) is only preserved from its medial side and shows the complete shape. The left

https://doi.org/10.1017/jpa.2023.58 Published online by Cambridge University Press

scapulocoracoid (Fig. 15.2–15.5) is visible in all views, but a few anterior and posteroventral parts are missing. The dorsal blade is taller in the mainly larger specimens of *Eryops*. The angle between the supraglenoid buttress and the anterior margin of the scapular blade varies from 90° on the right to slightly greater than 90° on the left scapulocoracoid of the paratypical *Stenokranio* n. gen. specimen. Such angles of 90° or slightly greater are typical of most *Eryops* specimens (Broili, 1899; Case, 1911; Romer, 1952; Langston, 1953; Pawley and Warren, 2006; RW, personal observation). One exception exists in *Eryops* in which the angle between these two structures is less than 90° (Williston, 1899, FMNH UR 756), but this may be due to post-mortem distortion. The angle between the supraglenoid buttress and the anterior margin of the scapular blade is less than 90°, and the coracoid region is longer in *Glaukerpeton* and *O. labyrinthicus* (Boy, 1990, fig. 5C). The dorsoventrally elongated subscapular fossa with both anterior–posterior directed supraglenoid foramen and coracoid foramen is particularly well seen as an oval depression on the narrow anterior side of the scapulocoracoid, while on its medial side it is hidden behind a sharp-angled ridge. The openings of the glenoid foramina can be observed from all four sides of the scapulocoracoid, but the largest depression is developed medially. The glenoid fossa is extended anterior-posteriorly through and demarcated by a bar-like ridge from the dorsally overlying triangular supraglenoid fossa with the lateral supraglenoid ridge and supraglenoid buttress as margins.

Etymology.—The species name honors the late Rudolf Bold from Rammelsbach near Kusel who found the holotype and only known specimen of the Remigiusberg sphenacodontid *Cryptovenator hirschbergeri* Fröbisch et al., 2011, in 2002 (Fröbisch et al., 2011).

Foreign tetrapod bones (Figs. 5, 6, 16).—A few bones in the palatal skull of the holotype of *Stenokranio boldi* n. gen. n. sp. are not assignable to the new eryopid because of their clearly smaller size or their greater robustness. These 'foreign tetrapod bones' may belong to a microsaur and a diadectomorph. Both tetrapod groups are known from additional material in the Remigiusberg lake sediments and detailed descriptions are in preparation.

?Microsaur.—The skull fragment is ~12 mm in length and bears a mandible with an ossified articular region and rounded posterior process(es) in dorsal view, and a dentary in lateral view. Its teeth have wide bases. One curved rib is 12 mm long. The probable humerus has rotated proximal and distal parts. In this bone, 7 mm of its length are preserved, but the full length may have been 10 mm. No entepicondylar foramen is preserved. The fully ossified pelvis in lateral view is 8–9 mm high, with a sutured ilium.

Diadectomorph.—A single phalanx with well-formed condyles is recorded. Its length is 11–12 mm.

Remarks.—None.

Phylogenetic relationships

Previous work.—In the last three decades, several authors have discussed the phylogenetic relationships of eryopids with other temnospondyl clades and yielded different results, however most of them can be assigned to one of two main concepts. In the first main concept, eryopids are the sister group of zatracheids and form the rather terrestrial clade Euskelia together with dissorophoids (Yates and Warren, 2000). This concept is based on phylogenetic hypotheses of Milner (1993) and Schoch (1997), in which eryopids, zatracheids, and dissorophoids likewise form monophyletic groups, but with different ingroup relationships (eryopids as sister group of dissorophoids in Milner, 1993; eryopids as sister group of zatracheids plus dissorophoids in Schoch, 1997). Among others, the shortened postorbital skull table, the sutural connection between parasphenoid and pterygoid in adults, and the proportionally less-elongate interclavicle compared to dvinosaurians and stereospondylomorphs were mentioned as supporting characters. However, Werneburg (2007) noted that an abbreviated skull table is not characteristic of all eryopids, and Witzmann et al. (2007) pointed to the fact that the proportions of the interclavicle in larval eryopids (*Onchiodon*) are comparable to those of adult stereospondylomorphs, rendering these synapomorphies doubtful and indicating a closer relationship of eryopids with stereospondylomorphs. This is the quintessence of the second concept, the Eryopiform hypothesis sensu Schoch (2013), which is based on the Eryopoidea hypothesis of Boy (1990). Indeed, the phylogenetic analyses of Schoch and Witzmann (2009a, b) and Schoch (2013, 2021a, b) found a sister-group relationship of eryopids and stereospondylomorphs. This grouping, named Eryopiformes by Schoch (2013), is characterized by proportionally large larval interclavicles and a "crocodyliform" skull with the anterior part of the jugal situated well anterior to the orbit (Schoch, 2013; Schoch and Milner, 2014).

In contrast to the phylogenetic relationships of eryopids with other temnospondyl clades, the intrarelationships of the group had long been neglected, although a large number of eryopid taxa have been described (Schoch and Milner, 2014). In previous works, no more than two or three different eryopid taxa have been considered in phylogenetic analyses (Boy, 1990; Schoch and Witzmann, 2009a; Werneburg and Berman, 2012; Schoch, 2013, 2021a). This gap was recently closed by the study of Schoch (2021b) on eryopid intrarelationships and ontogeny, which provided the first comprehensive phylogenetic analysis of almost all known valid eryopid taxa. The analysis found a monophyletic Eryopidae consisting of the successive sister taxa *Actinodon frossardi* Gaudry, 1866; *Osteophorus roemeri* Meyer, 1856; *Glaukerpeton avinoffi* Romer, 1952; *Onchiodon labyrinthicus* + *O. thuringiensis*, *Clamorosaurus nocturnus* Gubin, 1983; *Eryops* sp. from the Moran Formation, *Eryops anatinus* Broom, 1913; and *E. megacephalus*. A variant analysis including the incompletely known *Onchiodon langenhani* Werneburg, 1989, led to poorer resolution, with *O. langenhani* nesting between *Glaukerpeton avinoffi* and *Onchiodon* consisting of *O. labyrinthicus* plus *O. thuringiensis* (Schoch, 2021b).

Modifications to Schoch (2021b) matrix.—We included *Stenokranio boldi* n. gen. n. sp. in the recent phylogenetic analysis of Schoch (2021b) to elucidate the phylogenetic position of this new taxon. We deleted *Clamorosaurus nocturnus* because of some ambiguities in the original description (Gubin, 1983). *Clamorosaurus* currently is being

https://doi.org/10.1017/jpa.2023.58 Published online by Cambridge University Press

redescribed by two of the present authors (RW and FW). We also omitted two incompletely known taxa, the immature *Onchiodon langenhani* (Werneburg, 1989) and *Eryops anatinus* (Broom, 1913), which is probably also a juvenile specimen. Thus, our analysis is based on a total number of 26 taxa, including eight taxa referred to as eryopids. *Balanerpeton woodi* Milner and Sequeira, 1994, *Dendrerpeton helogenes* Steen, 1934 (Arbez et al., 2022; *Dendrysekos helogenes* sensu Schoch and Milner, 2014), and *Cochleosaurus bohemicus* (Fritsch, 1876) served as operational outgroups. We deleted six characters from the original matrix of Schoch (2021b) because of unclear definitions and/or partial redundancies. This refers to Schoch (2021b) characters #10, #15, #47, #57, #62, and #66.

We modified five characters of Schoch (2021b). Character #12 (#11 in the present study) as follows: "nasal (lateral margin): straight, longitudinal (0); stepped, with lateral excursion (1); or straight, oblique (2)" (revision based on Gee, 2022). Character #13 (#12 in the present study): "lacrimal (length): approximately as long as nasal (0), or shorter than nasal (1)." Character #26 (#24 in the present study): "jugal (anterior expansion): jugal does not reach level of anterior orbital margin in adults (0); jugal extends past orbit but does not reach level of anterior prefrontal margin (1); jugal reaches level of anterior prefrontal margin (2)." Character #29 (#27 in the present study): "vomerine tusks: anteromedial or medial to choana (0) or well anterior to choana (1)." Character #60 (#56 in the present study): "jugal width lateral to the orbit: wider than orbit (0) or markedly narrower (1)."

Two characters affecting the morphology of the postorbital and choana, respectively, were replaced by newly defined characters: #23 of Schoch (2021b) (#21 in the present analysis): "Postorbital: percentage of postorbital length to length of posterior skull table, measured in the midline from the level of the posterior orbital margin to the posterior end of postparietals. Postorbital part equal or more than 50% (0); less than 50% (1);" and #31 of Schoch (2021b) (#29 in the present study): "Choana (ratio length to width): ratio length to maximum width of choana between 2 and 3 (0); ratio smaller than 2 (1); ratio larger than 3 (2)."

We added four new characters, leading to a total of 70 characters. Character #67: "Width of interpterygoid vacuities through skull width on the level of orbital midlength larger or equal to 0.5 (0) or smaller (1)." Character #68: "length of interpterygoid vacuity divided by its width: larger or equal to 1 (0), or smaller than 1 (1)." Character #69: "distance of posterior choanal margin to anterior margin of interpterygoid vacuities (measured sagittally) less than half the length of the choana (0) or about half the length or more (1)." Character #70: "ratio skull length (measured from the tip of premaxilla to posterior end of postparietals) through posterior width of skull at level of posterolateral margins of cheeks: larger than 1 (0); smaller or equal to 1 (1)."

Numerous character states in the matrix of Schoch (2021b) had to be recoded for the present analysis, either because of scoring errors or because of the reformulation of certain characters. In the following, the rescored characters and the affected taxa are listed. Characters #19, #24, and #29 are ordered, all other characters are unordered. The numbering of characters refers to the present study; the numbers given in square brackets refer to the original numbering in Schoch (2021b), if different. The complete list of characters and the character-taxon matrix are given in Supplementary Information 1 and 2.

Dendrerpeton helogenes.—#2-1; #7-1; #17-1 [#19]; #24-1 [#26] (Arbez et al., 2022).

Balanerpeton woodi.—#11-1 [#12]; #12-1 [#13] (Schoch and Milner, 2014).

Cochleosaurus bohemicus.—#7-0/1; #14-1 [#16]; #17-1 [#19]; #24-1 [#26]; #38-1 [#40] (Sequeira, 2004).

Micromelerpeton credneri *Bulman and Whittard, 1926*.—#11-1 [#12]; #12-1 [#13]; #65-1 [#71] (Schoch and Milner, 2014).

Acanthostomatops vorax *(Credner, 1883)*.—#11-2 [#12]; #24-1 [#26]; #27-1 [#29]; #29-1 [#31]; #65-1 [#71] (Schoch and Milner, 2014).

Iberospondylus schultzei *Laurin and Soler-Gijón, 2001*.—#18-1 [#20]; #24-1 [#26]; #29-2 [#31] (Laurin and Soler-Gijón, 2006).

Actinodon frossardi.—#2-1; #21-1 [#23]; #65-1 [#71] (Werneburg, 1997; Werneburg and Steyer, 1999).

Osteophorus roemeri.—#2-1; #11-1 [#12] (Meyer, 1860a).

Glaukerpeton avinoffi.—#2-1; #11-1 [#12]; #24-2 [#26]; #29-1 [#31]; #65-1 [#71] (Werneburg and Berman, 2012).

Onchiodon labyrinthicus.—#2-1; #11-1 [#12]; #29-1 [#31]; #44-0/1 [#46] (Boy, 1990).

Onchiodon thuringiensis.—#2-1; #21-0 [#23]; #24-2 [#26]; #29-1 [#31] (Werneburg, 2007).

Eryops megacephalus.—#2-1; #11-1 [#12]; #12-1 [#13]; #21-0 [#23]; #24-2 [#26]; #29-1 [#31]; #44-1 [#46] (Sawin, 1941; Schoch and Milner, 2014).

Eryops *sp. from the Moran Formation*.—#11-1 [#12]; #12-1 [#13]; #21-0 [#23]; #24-2 [#26]; #29-1 [#31]; #44-1 [#46] (Werneburg, 2007; Schoch and Milner, 2014).

Sclerocephalus stambergi *Klembara and Steyer, 2012*.—#2-?; #11-0/1 [#12]; #12-0 [#13]; #21-1 [#23]; #24-1 [#26]; #65-? [#71] (Klembara and Steyer, 2012).

Sclerocephalus bavaricus *Branco, 1887*.—#12-1 [#13]; #17-1 [#19]; #27-? [#29]; #29-? [#31]; #44-? [#46] (Boy, 1988; Schoch and Witzmann, 2009a).

Sclerocephalus haeuseri *Goldfuss, 1847*.—#11-1 [#12]; #12-1 [#13]; #17-1 [#19]; #18-0/1 [#20] (Boy, 1988; Schoch and Witzmann, 2009a).

Sclerocephalus concordiae *Schoch and Sobral, 2021*.—#11-1 [#12]; #12-1 [#13]; #17-1 [#19]; #65-1 [#71] (Schoch and Sobral, 2021).

Glanochthon angusta *Schoch and Witzmann, 2009b, and* G. latirostre *(Jordan, 1849a)*.—#12-0/1 [#13]; #17-1 [#19]; #27-1 [#29]; #29-2 [#31] (Schoch and Witzmann, 2009b).

https://doi.org/10.1017/jpa.2023.58 Published online by Cambridge University Press

Intasuchus silvicola *Konzhukova, 1956*.—#9-0; #17-1 [#19]; #18-1 [#20]; #29-2 [#31] (Werneburg et al., 2020).

Melosaurus uralensis *Meyer, 1857*.—#12-1 [#13]; #17-1 [#19]; #21-1 [#23]; #29-2 [#31] (Meyer, 1860b; Hartmann-Weinberg, 1939).

Cheliderpeton vranyi *Fritsch, 1877*.—#2-1; #17-1 [#19]; #21-1 [#23]; #54-0/1 [#58]; #55-1 [#59] (Werneburg and Steyer, 2002).

Archegosaurus decheni *Goldfuss, 1847*.—#17-1 [#19]; #27-0 [#29]; #29-2 [#31]; #65-1 [#71] (Witzmann, 2006).

Platyoposaurus stuckenbergi *(Trautschold, 1884)*.—#12-1 [#13]; #17-1 [#19] (Gubin, 1991).

Australerpeton cosgriffi *Barberena, 1998*.—#1-0; #12-1 [#13]; #17-1 [#19]; #29-2 [#31]; #49-0 [#52]; #50-2 [#53] (Eltink and Langer, 2014; Eltink et al., 2016).

Results using modified, updated matrix.—The analysis was conducted with PAUP 3.1/MacClade 3.0 (Swofford, 1991; Maddison and Maddison, 1992) in the heuristic mode with branch swapping (TBR) options, using random addition sequence replicates (number of replicates = 1000). The analysis yielded 56 most parsimonious trees. The tree length is 172, the consistency index CI = 0.4419, and the retention index RI = 0.7405. The resulting strict consensus tree is shown in Figure 20. The strict consensus of the eryopid intrarelationships is illustrated in Figure 21. Additionally, a parsimony bootstrap analysis with heuristic search under the same setting was performed using 200 bootstrap replicates.

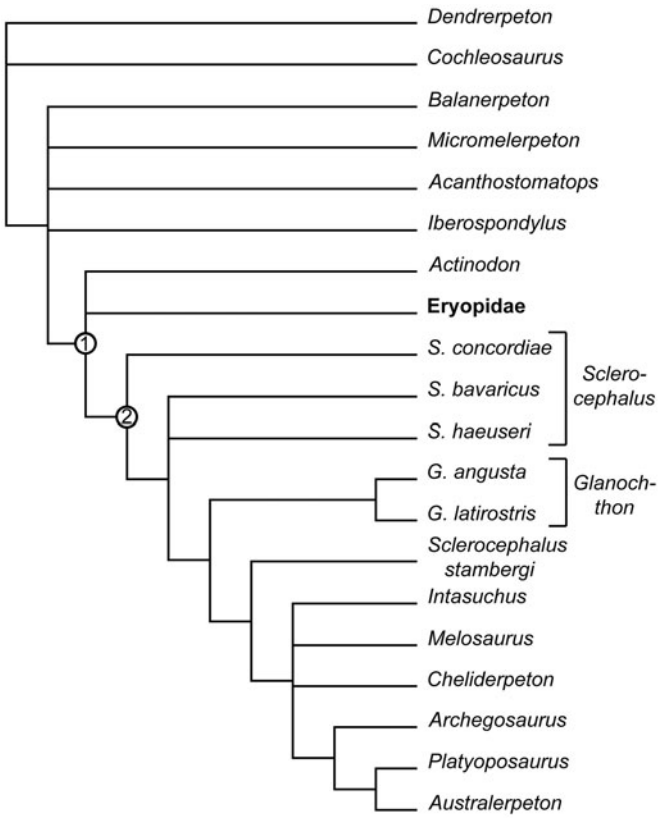

Figure 20. Phylogenetic position of the Eryopidae within temnospondyls. Strict consensus tree of 56 most parsimonious trees. The intrarelationships of the Eryopidae are shown in Figure 21. 1 = Eryopiformes; 2 = Stereospondylomorpha.

The present analysis found a monophyletic Eryopidae (bootstrap 80%) as the sister group to Stereospondylomorpha, thus supporting the Eryopiformes hypothesis. However, in contrast to previous analyses, the position of *Actinodon frossardi* is not resolved. This taxon may fall outside Eryopidae as a basal stereospondylomorph. This unusual position is supported by one unambiguous synapomorphy: the interclavicle being longer than half the skull length (#43-1). Nevertheless, the bootstrap analysis found *Actinodon frossardi* as the basalmost eryopid, as revealed by the analysis of Schoch (2021b), albeit poorly supported (bootstrap support of 49%). The Eryopidae (with *Actinodon* excluded) is supported by two unique derived characters: the posterolaterally expanded lateral suture of the lacrimal (#13-1) and the length of the posterior skull table measuring 0.4–0.6 times the width (#19-3). Five further derived, but non-unique characters are: the frontal being shorter than the nasal (#16-1, shared with *Cochleosaurus* Fritsch, 1885; *Intasuchus* Konzhukova, 1956; *Melosaurus* Meyer, 1857; *Cheliderpeton* Fritsch, 1877; *Archegosaurus* Goldfuss, 1847; *Platyoposaurus* Lydekker, 1889; and *Australerpeton* Barberena, 1998); the interorbital distance being wider than the orbital width (#17-1; shared with *Acanthostomatops* Kuhn, 1961, and *Actinodon*); a tightly sutured basicranial articulation in adults (#36-1, shared with *Sclerocephalus concordiae* and *Australerpeton*); the straight, posterodorsally directed shaft of the ilium (#50-2, shared with *Acanthostomatops* and *Australerpeton*); and the short lacrimal (#58-1, reversal in *O. labyrinthicus*, shared with *S. bavaricus*, *S. haeuseri*, *S. concordiae*, *Glanochthon* Schoch and Witzmann, 2009b, and *Cheliderpeton*).

The three basalmost eryopids, *Osteophorus roemeri*, *Glaukerpeton avinoffi*, and *Onchiodon labyrinthicus*, form an unresolved polytomy. The clade consisting of *Onchiodon thuringiensis*, *Stenokranio boldi* n. gen. n. sp., *Eryops megacephalus*, and *Eryops* sp. from the Moran Formation is supported by the following three apomorphies (bootstrap 82%): the long postorbital (#21-0, shared with *Iberospondylus* Laurin and Soler-Gijón, 2001, and sterospondylomorphs except for *S. stambergi*, *Melosaurus*, and *Cheliderpeton*); the fully ossified neurocranium (#53-1, shared with *S. concordiae* and reversal in *Stenokranio* n. gen.); and the slender interpterygoid vacuities (#67-1, shared with *Platyoposaurus*).

The next clade, comprising *Stenokranio boldi* n. gen. n. sp. and the two species of *Eryops*, possesses three apomorphies (bootstrap 66%): the lacrimal being shorter than the nasal (#12-1, shared with *Balanerpeton* Milner and Sequeira, 1994, *Micromelerpeton* Bulman and Whittard, 1926, and stereospondylomorphs except for *S. stambergi*, *Intasuchus*, *Cheliderpeton*, and *Archegosaurus* [both *Glanochthon* species are polymorphic in this respect]); the ectopterygoid fangs being similar to palatine fangs (#66-0, reversal with respect to *Onchiodon thuringiensis* and *O. labyrinthicus*); and the slender skull (#70-0, shared with *Dendrerpeton* Owen, 1853, *Cochleosaurus*, *Micromelerpeton*, *Iberospondylus*, and all stereospondylomorphs except *S. concordiae* and the genus *Eryops*—represented here by *E. megacephalus* and the still undescribed species from the

https://doi.org/10.1017/jpa.2023.58 Published online by Cambridge University Press

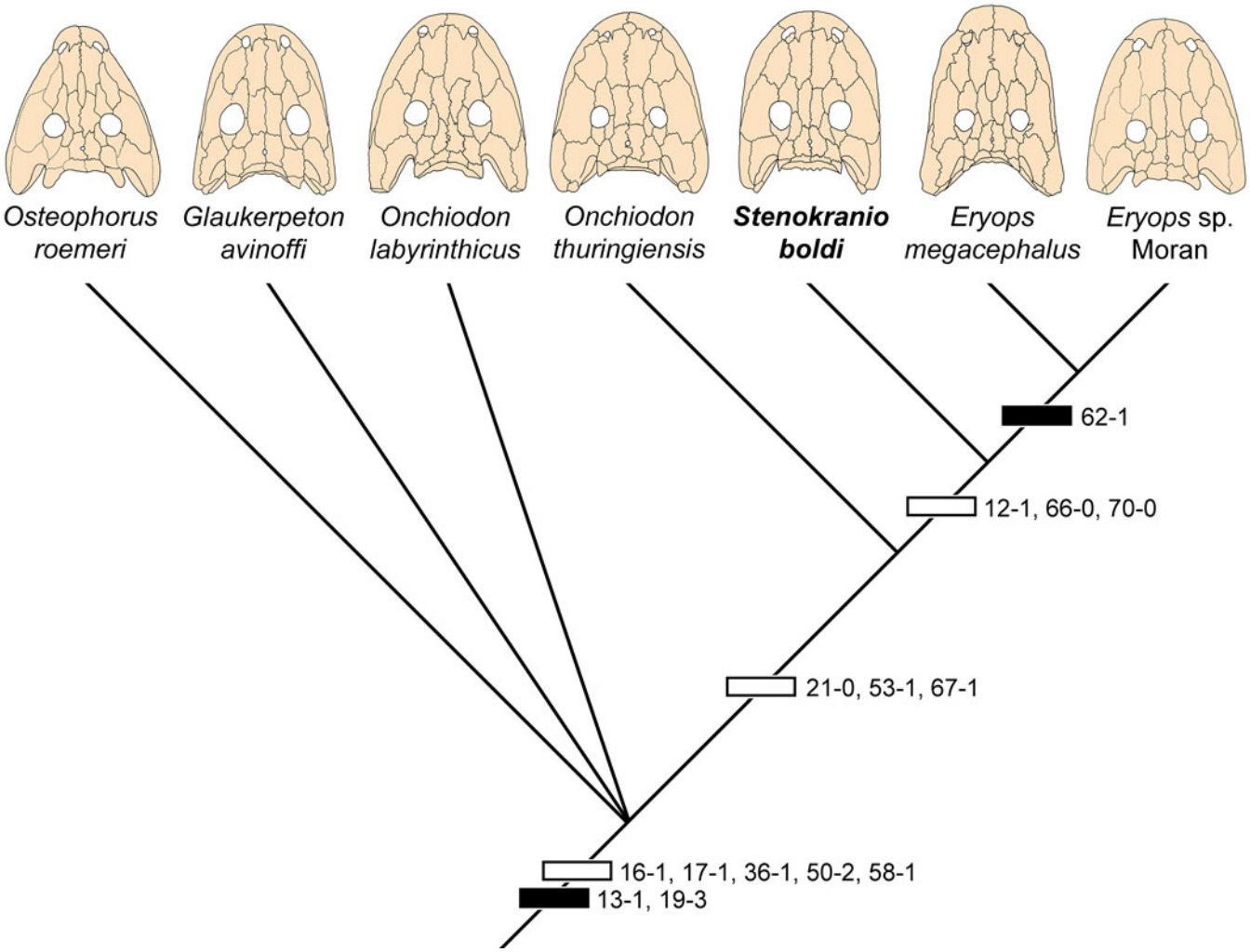

Figure 21. Intrarelationships of the different species of Eryopidae. Strict consensus tree of 56 most parsimonious trees. Supporting characters are mapped on nodes, with synapomorphies represented by black and homoplasies by white rectangles. The numbers refer to the characters listed in Supplementary Information 1.

Moran Formation (Werneburg, 2007; Schoch and Milner, 2014; Schoch, 2021b)—possesses one unambiguous synapomorphy, the septomaxilla without dorsal exposure (#62-1) (bootstrap 74%).

Summary of phylogenetic relationships.—Although the Eryopidae is well supported as a clade, it is striking that those taxa that were found as the most basal representatives of the group by Schoch (2021b) may be either a basal stereospondylomorph (in the case of *Actinodon*) or form a polytomy at the base of the Eryopidae (*Osteophorus* and *Glaukerpeton* with *Onchiodon labyrinthicus*). An interesting result of the present study is that *Onchiodon* is either polyphyletic or paraphyletic, with *O. labyrinthicus* being in a more basal position and *O. thuringiensis* being the sister group to *Stenokranio* n. gen. and *Eryops*. If this grouping is correct, then the small ectopterygoid fangs, regarded as an autapomorphy of the genus by Werneburg (2007) and Schoch (2021b), evolved in parallel in *O. labyrinthicus* and *O. thuringiensis*. However, we refrain from removing *O. thuringiensis* from the genus *Onchiodon*, awaiting a more comprehensive analysis of eryopids that includes new descriptions of the eryopids from Russia (Werneburg and Witzmann, in prep.) and the Intrasudetic Basin (Werneburg, 1993). The large number of homoplastic characters of eryopids with stereospondylomorphs and especially with the zatracheid *Acanthostomatops* is striking and can be attributed to a high degree of parallel evolution, especially in the similar construction of a widened skull with a relatively elongated snout (as in stereospondylomorphs and zatracheids) and the shortened pectoral girdle (as in zatracheids).

Paleoecology

The *Stenokranio* n. gen. skulls and preserved postcrania fit the known eryopid bauplan. Eryopid skeletons are conservative in their general proportions (Pawley and Warren, 2006), therefore, assumptions that *Stenokranio* n. gen. was similar in appearance to *Eryops megacephalus* (Case, 1911), and *Onchiodon thuringiensis* Werneburg, 2007, are plausible. *Stenokranio* n. gen. was a medium-sized temnospondyl (skull size at least 27 cm) whose adults probably reached a length of up to 150 cm, thus it was within the size range of *Onchiodon* (Werneburg, 2007).

https://doi.org/10.1017/jpa.2023.58 Published online by Cambridge University Press

The large fangs and numerous smaller teeth clearly indicate a carnivorous diet. Based on the rostral morphology protocols of Busby (1995, fig. 10.2) the rostrum of *Stenokranio* n. gen. was alligator-like and may indicate generalist feeding, especially as recent studies show temnospondyls were capable of more than one feeding strategy (e.g., Fortuny et al., 2016, Konietzko-Meier et al., 2018). The mesiodistally developed carinae on the upper tooth parts (Fig. 12.2) together with the closely packed teeth seem best suited to hold slippery prey, to initiate penetration, to propagate cracks in hard tissue, and to cut through the food item (Rinehart and Lucas, 2013; Fortuny et al., 2016). Capturing was most likely made by some lateral movement of the head or an aggressively forward strike of the whole body (Witzmann, 2005) since the lack of a significant neck limited a single thrust of the head forward (Rinehart and Lucas, 2013). But the wider jaw and weaker symphysis of *Stenokranio* n. gen. would not have allowed the violent side-to-side shaking that modern crocodilians use to subdue prey (Walmsley et al., 2013). As with other eryopids (Schoch, 2009a), prey may have included predominantly aquatic animals such as fish, freshwater sharks, and amphibians, but terrestrial tetrapods such as synapsid edaphosaurs and sphenacodontids were not excluded (Werneburg, 2007; Flies et al., 2019). Moreover, cannibalism (Bakker, 1982; Flies et al., 2019), as documented in other fossil temnospondyls such as *Mastodonsaurus* Jaeger, 1828 (Schoch and Seegis, 2016), *Sclerocephalus* (Schoch, 2014), and branchiosaurids (Werneburg, 1989; Witzmann, 2009), seems likely.

Stenokranio n. gen. shows signs of both terrestrial and aquatic adaptation, as known and debated from other eryopids (e.g., Pawley, 2006; Sanchez et al., 2010; Fortuny et al., 2011, 2016; Quemeneur et al., 2013; Konietzko-Meier et al., 2016; Carter et al., 2021, Herbst et al., 2022). Its terrestrial adaptions include a massive, highly ossified shoulder girdle (Pawley and Warren, 2006; Schoch, 2009a), uncinate processes to strengthen the rib cage (Boy, 2007; Quemeneur et al., 2013), intercentra that indicate terrestriality according to geometric morphometric comparisons (Carter et al., 2021), absence of external lateral line sulci (Boy, 1990; Werneburg, 2007), absence of an ossified branchial system (Witzmann, 2005), and presence of large tympanic ears with rodlike stapes for receiving high-frequency sound (Pawley and Warren, 2006). Geometric morphometric analysis of the skull stress during feeding using finite element analysis (FEA) and principal components analysis (PCA) (Fortuny et al., 2011) provides additional evidence of terrestrial feeding capability.

Apparent aquatic adaptations include eyes and nostrils that were dorsally located, as in modern crocodiles, to permit stealthy approach of prey (Case, 1911; Pawley, 2006); laterally expanded ribs that might be related to swimming locomotion (Cowan, 1996); and sharp, closely packed teeth that may indicate at least some piscivory. Thus, *Stenokranio* n. gen. probably was, like *Onchiodon* (Fortuny et al., 2016), semiaquatic. This allowed the advantages of a wider food range, travel to new water sources, or the ability to change habitats (e.g., for reproduction [Schoch, 2014]), and for habitat shifts of juveniles and adults (Bakker, 1982; Boy, 1990; Witzmann, 2005).

The habitat of *Stenokranio* n. gen. was probably the marginal lacustrine paleoenvironment of the Theisbergstegen lake of the Remigiusberg Formation. However, it is possible, though unlikely because of the number of *Stenokranio* n. gen. finds in the Remigiusberg quarry, that the remains are allochthonous, and its home was more upland (Witzmann and Voigt, 2014). *Stenokranio* n. gen. is associated with a variety of aquatic, semiaquatic, and terrestrial taxa (Voigt et al., 2019), such as sarcopterygian fishes, palaeonisciformes, acanthodians, freshwater sharks (*Triodus* Jordan, 1849b; *Lebachacanthus* Heidtke, 1998; Voigt et al., 2014), "lepospondyls" (lysorophids, "microsaurs," urocordylids; Boy and Schindler, 2000), a trimerorhachid-like dvinosaur (*Trypanognathus remigiusbergensis* Schoch and Voigt, 2019), diadectomorphs (Voigt et al., 2019), a synapsid edaphosaurid (*Remigiomontanus robustus* Spindler et al., 2020), and a synapsid sphenacodontid (*Cryptovenator hirschbergeri* Fröbisch et al., 2011). This faunal assemblage is largely in accordance on the genus level with vertebrate communities from the Pennsylvanian–Permian of North America (e.g., Case, 1915; Romer, 1928; Olson, 1958; Sander, 1987; Johnson, 2011; Shelton et al., 2013; Davis, 2018) and the early Permian of Germany (Werneburg, 2007; Schneider et al., 2010). The fossil record also indicates that *Stenokranio* n. gen. and fellow eryopids occupied their habitats exclusively (Witzmann and Voigt, 2014), which precluded other large temnospondyls such as *Sclerocephalus*, and vice versa. Coexistence of two carnivorous predators of the same size (Schoch, 2009b) and with the same habitat requirements (Boy, 2007; Schoch, 2014; Schoch and Milner, 2014) seems not to have been permitted by the natural resources. Except for some food specialists, such a distinct taxon separation is known, for example, in modern crocodilians (Peters, 1991). A complementary exclusion criterion might have been varying water levels and derived living conditions in the Remigiusberg environment, depending on dry and rainy seasons of a monsoonal climate (Voigt et al., 2019), that required different hunting techniques (Konietzko-Maier et al., 2018). *Stenokranio* n. gen., as a less-specialized predator, may have been better adapted than the predominantly piscivorous *Sclerocephalus* (Boy, 2007; Schoch, 2009a). The latter also would have had to rival the large piscivorous freshwater shark *Lebachacanthus* (Schoch, 2009a).

Conclusions

Based on the new eryopid specimens, we arrive at seven conclusions. (1) *Stenokranio boldi* n. gen. n. sp. was found in fluviolacustrine deposits of the latest Carboniferous–earliest Permian (Gzhelian/Asselian) Remigiusberg Formation at the Remigiusberg quarry near Kusel, Saar–Nahe Basin, southwest Germany. The holotypic specimen was preserved in a dark grayish unbedded carbonaceous mudstone with abundant intraformational pebbles interpreted to represent mudflow deposition in a shallowly subaquatic lacustrine paleoenvironment. The other described (paratypic) specimen was found in greenish phytoturbated massive mudstone of a supposed lake shoreline paleoenvironment. (2) *Stenokranio boldi* n. gen. n. sp. clearly belongs to the family Eryopidae with five of the seven diagnosed synapomorphies. Three autapomorphies distinguish *Stenokranio* n. gen. from all other eryopid genera: the posterior part of the skull is distinctly narrow, and therefore the skull has nearly parallel lateral margins; the postparietals and tabulars form a short bony strip, therefore the parietals reach posteriorly nearly

https://doi.org/10.1017/jpa.2023.58 Published online by Cambridge University Press

to a common transverse line with the posterior margin of the short supratemporals; and the ectopterygoid is very wide, its most posterior part and the neighboring pterygoid are equal in width. (3) The mandible of *Stenokranio boldi* n. gen. n. sp. presents six significant differences to an isolated eryopid mandible (POL-F 2012-001), which also was found at the locus typicus Remigiusberg quarry and was reported by Witzmann (2013). Therefore, probably two different eryopids are known from Remigiusberg. (4) A few "foreign tetrapod bones" in the palatal skull of the holotype from *Stenokranio boldi* n. gen. n. sp. may belong to a small microsaur and a middle-sized diadectomorph. These bones possibly belonged to earlier captured prey animals, or were accidentally embedded under the skull of *Stenokranio* n. gen. (5) A phylogenetic analysis finds a monophyletic Eryopidae with the basal taxa *Osteophorus*, *Glaukerpeton*, and *Onchiodon labyrinthicus* forming a polytomy. The status of *Actinodon* is not clear—it may either be a basal eryopid or stereospondylomorph. *Stenokranio* n. gen. is found as a more derived eryopid forming the sister taxon to *Eryops*. Interestingly, the genus *Onchiodon* is not monophyletic in the present study, but we refrain from removing *O. thuringiensis* from the genus *Onchiodon*, awaiting a more comprehensive description and analysis of the eryopids from Russia and the Intrasudetic Basin (Werneburg, 1993). The remarkably large number of homoplastic characters in the skull shared by eryopids, stereospondylomorphs and zatracheids may be ascribed to a high degree of parallel evolution of a broad skull with an elongate, crocodile-like snout. (6) *Stenokranio boldi* n. gen. n. sp. was part of a characteristic faunal assemblage of aquatic, semiaquatic, and terrestrial vertebrates that is also known in higher-taxon compositions from other late Carboniferous–early Permian localities of Germany and North America. (7) *Stenokranio boldi* n. gen. n. sp. was among the largest predators of Carboniferous–Permian time in the Saar–Nahe Basin. Its semiaquatic lifestyle enabled *Stenokranio* n. gen. to browse riverbanks and lake shorelines for prey, but it probably hunted aquatic vertebrates. As a generalized feeder, *Stenokranio boldi* n. gen. n. sp. was perfectly adapted to the changing environmental conditions caused by rainy and dry seasons at the time of Theisbergstegen lake environment.

Acknowledgments

G. Sommer, Schleusingen, is appreciated for skillful preparation of the ventral side of the holotype of the new eryopid. For access to the Remigiusberg quarry and logistic support, we are thankful to the Basalt AG and former and local operation managers O. Schneider and K. Schön, respectively. We appreciate field assistance and other help by T. Bach, W. Conrath, O. Emrich, H.-R. Matzenbacher, and H. Rapin. Fossil excavations at the Remigiusberg quarry are conducted under the permission of the Bureau for the Conservation of Historic Monuments in the state of Rhineland–Palatinate (Generaldirektion Kulturelles Erbe Rheinland-Pfalz). D. Marjanović is thanked for help with the phylogenetic analysis. Financial support for field work and laboratory work was given by the Palatinate Museum of Natural History (Pfalzmuseum für Naturkunde – POLLICHIA-Museum), whose geoscientific branch is the Urweltmuseum GEOSKOP. We appreciate careful and constructive reviews of Bryan Gee and an anonymous reviewer.

Declaration of competing interests

The authors declare that they have no competing interests.

Data availability statement

Data available from the Zenodo Digital Repository: https://doi.org/10.5281/zenodo.8298571.

References

Arbez, T., Atkins, J.B., and Maddin, H.C., 2022, Cranial anatomy and systematics of *Dendrerpeton* cf. *helogenes* (Tetrapoda, Temnospondyli) from the Pennsylvanian of Joggins, revisited through micro-CT scanning: Papers in Palaeontology, v. 8, e1421, https://doi.org/10.1002/spp2.1421.

Bakker, R.T., 1982, Juvenile–adult habitat shift in Permian fossil reptiles and amphibians: Science, v. 217, p. 53–55.

Barberena, M.C., 1998, *Australerpeton cosgriffi* n. g., n. sp., a late Permian rhinesuchoid amphibian from Brazil: Anais da Academia Brasileira des Ciencias, v. 70, p. 125–137.

Boy, J.A., 1988, Über einige Vertreter Eryopoidea (Amphibia: Temnospondyli) aus dem europäischen Rotliegend (?höchstes Karbon–Perm) 1. *Sclerocephalus*: Paläontologische Zeitschrift, v. 62, p. 107–132.

Boy, J.A., 1990, Über einige Vertreter der Eryopoidea (Amphibia: Temnospondyli) aus dem europäischen Rotliegend (?höchstes Karbon–Perm) 3. *Onchiodon*: Paläontologische Zeitschrift, v. 64, p. 287–312.

Boy, J.A., 2007, Als die Saurier noch klein waren: tetrapoden im Permokarbon, *in* Schindler, T., and Heidtke, U.H.J., eds., Kohlesümpfe, Seen und Halbwüsten. Dokumente einer rund 300 Millionen Jahre alten Lebewelt zwischen Saarbrücken und Mainz: POLLICHIA–Sonderveröffentlichung, v. 10, p. 258–286.

Boy, J.A., and Schindler, T., 2000, Ökostratigraphische bioevents im Grenzbereich Stephanium/Autunium (höchstes Karbon) des Saar–Nahe–Beckens (SW-Deutschland) und benachbarter Gebiete: Neues Jahrbuch für Geologie und Paläontologie, Abhandlungen, v. 216, p. 89–152.

Boy, J.A., Haneke, J., Kowalczyk, G., Lorenz, V., Schindler, T., Stollhofen, H., and Thum, H., 2012, Rotliegend im Saar–Nahe–Becken, am Taunus–Südrand und im nördlichen Oberrheingraben: Schriftenreihe der Deutschen Gesellschaft für Geowissenschaften, v. 61, p. 254–377.

Branco, W., 1887, *Weissia bavarica* g. n. sp. n., ein neuer Stegocephale aus dem unteren Rotliegenden: Jahrbuch der Königlich-Preussischen Geologischen Landes-Anstalt und Bergakademie Berlin, v. 1886, p. 22–39.

Broili, F., 1899, Ein Beitrag zur Kenntnis von *Eryops megacephalus* Cope: Palaeontographica, v. 46, p. 61–84.

Broom, R., 1913, Studies on the Permian temnospondylous Stegocephalia of North America: Bulletin of the American Museum of Natural History, v. 32, p. 563–595.

Bulman, O.M.B., and Whittard, W.F., 1926, On *Branchiosaurus* and allied genera: Proceedings of the Zoological Society London, v. 1926, p. 533–579.

Burger, K., Hess, J.C., and Lippolt, H.J., 1997, Tephrochronologie mit kaolin–kohlentonsteinen: mittel zur korrelation paralischer und limnischer Ablagerungen des Oberkarbons: Geologisches Jahrbuch, v. A147, p. 3–39.

Busby, A.B., 1995, The consequences of skull flattening in crocodilians, *in* Thomason, J.J., ed., Functional Morphology in Vertebrate Paleontology: New York, Cambridge University Press, p. 173–192.

Carter, A.M., Hsieh, S.T., Dodson, P., and Sallan, L., 2021, Early amphibians evolved distinct vertebrae for habitat invasions: PloS ONE, v. 16, e0251983, https://doi.org/10.1371/journal.pone.0251983.

Case, E.C., 1911, Revision of the Amphibia and Pisces of the Permian of North America: Publications of the Carnegie Institute Washington, v. 146, p. 1–179.

Case, E.C., 1915, Permo-Carboniferous red beds of North America and their vertebrate fauna: Publications of the Carnegie Institution of Washington, v. 207, p. 1–176.

Cope, E.D., 1878, Descriptions of extinct Vertebrata from the Permian and Triassic formations of the United States: Proceedings of the American Philosophical Society, v. 17, p. 182–195.

Cope, E.D., 1882, The rhachitomous Stegocephalia: American Naturalist, v. 16, p. 334–335.

Cope, E.D., 1888, On the shoulder girdle and extremities of *Eryops*: Transactions of the American Philosophical Society, v. 16, p. 362–367.

Cowan, R., 1996, Locomotion and respiration in aquatic airbreathing vertebrates, *in* Jablonski, D., Erwin, D.H., and Lipps, J.H., eds., Evolutionary Paleobiology: Chicago, University of Chicago Press, p. 337–354.

Credner, H., 1883, Die Stegocephalen aus dem Rothliegenden des Plauen'schen Grundes bei Dresden. Vierter theil: Zeitschrift der Deutschen Geologischen Gesellschaft, v. 35, p. 275–300.

Davis, K., 2018, The Lower Permian Vertebrate Fauna of Waurika, Oklahoma: Kieran Davis, 684 p. [available at https://www.rhyniechert.com/permian/waurika_oklahoma]

Eltink, E., and Langer, M.C., 2014, A new specimen of the temnospondyl *Australerpeton cosgriffi* from the late Permian of Brazil (Rio do Rasto Formation, Paraná Basin): comparative anatomy and phylogenetic relationships: Journal of Vertebrate Paleontology, v. 34, p. 524–538.

Eltink, E., Dias, E.V., Dias-da-Silva, S., Schultz, C.L., and Langer, M.C., 2016, The cranial morphology of the temnospondyl *Australerpeton cosgriffi* (Tetrapoda: Stereospondyli) from the Middle–Late Permian of Paraná Basin and the phylogenetic relationships of Rhinesuchidae: Zoological Journal of the Linnean Society, v. 176, p. 835–860.

Flies, C.J., Bakker, R.T., Flis, J.E., Hass, M.M., and Cook, L.A., 2019, Adult *Eryops*, largest semi-aquatic apex predators of the Texas red beds, Lower Clear Fork, preferred fast flowing streams, preying upon edaphosaurs, dimetrodonts and other *Eryops*: Geological Society of America, Abstracts with Programs, v. 51, paper no. 38-12, https://doi.org/10.1130/abs/2019AM-338295.

Fortuny, J., Marcé-Nogué, J., Esteban-Trivigno, S. De, Gil, L., and Galobart, À, 2011, Temnospondyl bite club: ecomorphological patterns of the most diverse group of early tetrapods: Journal of Evolutionary Biology, v. 24, p. 2040–2054.

Fortuny, J., Marcé-Nogué, J., Steyer, J.-S., de Esteban-Trivigno, S., Mujal, E., and Gil, L., 2016, Comparative 3-D analysis and palaeoecology of giant early amphibians (Temnospondyli: Stereospondyli): Scientific Reports, v. 6, 30387, https://doi.org/10.1038/srep30387.

Fritsch, A., 1876, Über die Fauna der Gaskohle des Pilsner und Rakonitzer Beckens: Sitzungsberichte der Königlich-Böhmischen Akademie der Wissenschaften Prag, v. 1875, p. 70–79.

Fritsch, A., 1877, Über einen neuen Saurier aus den Kalksteinen der Permformation (U. Dyas) aus Braunau in Böhmen: Verlag der Königlich Böhmischen Gesellschaft der Wissenschaften, v. 1877, p. 1–3.

Fritsch, A., 1885, Fauna der Gaskohle und der Kalksteine der Permformation Böhmens: v. 2, Prague.

Fröbisch, J., Schoch, R.R., Müller, J., Schindler, T., and Schweiss, D.J., 2011, A new basal sphenacodontid synapsid from the Late Carboniferous of the Saar–Nahe Basin, Germany: Acta Palaeontologica Polonica, v. 56, p. 113–120.

Gaudry, A., 1866, Sur le reptile découvert par M. Frossard, à la partie supérieure du terrain houllier de Muse, près Autun (Saône-et-Loire): Comptes Rendus Hebdomadeires de l'Académie des Sciences Paris, v. 63, p. 341–344.

Gee, B.M., 2022, The disadvantage of derivation: conserved systematic flaws in primary data have repeatedly biased the phylogenetic inference of Temnospondyli (Tetrapoda, Amphibia): BioRχiv, https://doi.org/10.1101/2022.06.22.496729. [preprint, not certified by peer review]

Geinitz, H.B., 1862, Dyas oder die Zechsteinformation und das Rotliegende: Teile 1–18, Selbstverlag, Dresden.

Goldfuss, A., 1847, Goldfuss, A., 1847, Beiträge zur vorweltlichen Fauna des Steinkohlengebirges: Bonn, Naturhistorischer Verein der Preussischen Rheinlande, 26 p.

Gubin, Y.M., 1983, [The first eryopids from the Permian of the East-European Platform]: Palaeontologiceskij Zhurnal, v. 1983, p. 110–115. [in Russian]

Gubin, Y.M., 1991, [Permian archegosauroid amphibians of the USSR]: Trudy Paleontologichesko Instituta Nauka SSSR, v. 249, p. 1–138. [In Russian]

Hartmann-Weinberg, A.P., 1939, *Melosaurus uralensis* H. v. M., an Upper Permian archegosaurid: Problems in Paleontology, v. 5, p. 7–31.

Heidtke, U.H.J., 1998, Revision der Gattung *Orthacanthus* Agassiz 1843 (Chondrichthyes: Xenacanthida): Paläontologische Zeitschrift, v. 72, p. 135–147.

Herbst, E.C., Manafzadeh, A.R., and Hutchinson, J.R., 2022, Multi-joint analysis of pose viability supports the possibility of salamander-like hindlimb configurations in the Permian tetrapod *Eryops megacephalus*: Integrative and Comparative Biology, v. 62, p. 139–151.

Jaeger, G.F., 1828, Über Die Fossile Reptilien, Welche in Württemberg Aufgefunden Worden Sind: Stuttgart, Metzler.

Jaekel, O., 1909, Über die Klassen der Tetrapoden: Zoologischer Anzeiger, v. 34, p. 193–212.

Johnson, G.D., 2011, Lower–Middle Permian Vertebrates of Texas. Guidebook Poster-conference Field Trip: 12th International Symposium on Early Vertebrates/Lower Vertebrates, 15–18 June 2011: Dallas, Texas, Southern Methodist University, 54 p.

Jordan, H., 1849a, Ergänzende beobachtungen zu der abhandlung von Goldfuss über die gattung *Archegosaurus*: Verhandlungen des naturhistorischen Vereins für Rheinlande und Westphalen, v. 6, p. 76–81.

Jordan, H., 1849b, Triodus sessilis, *ein neuer Fisch der Kohlenformation von Lebach*: Neues Jahrbuch für Mineralogie, Geologie und Paläontologie, Bonn, p. 843.

Klembara, J., and Steyer, J.S., 2012, A new species of *Sclerocephalus* (Temnospondyli: Stereospondylomorpha) from the early Permian of the Boskovice Basin (Czech Republic): Journal of Paleontology, v. 86, p. 302–310.

Konietzko-Meier, D., Shelton, C.D., and Sander, P.M., 2016, The discrepancy between morphological and microanatomical patterns of anamniotic stegocephalian postcrania from the Early Permian Briar Creek Bonebed (Texas): Comptes Rendues Palevol, v. 15, p. 103–114.

Konietzko-Meier, D., Gruntmejer, K., Marcé-Nogué, J., Bidzioch, A., and Fortuny, J., 2018, Merging cranial histology and 3D-computational biomechanics: a review of the feeding ecology of a Late Triassic temnospondyl amphibian: PeerJ, v. 6, e4426, https://doi.org/10.7717/peerj.4426.

Konzhukova, E.D., 1956, (The Intan lower Permian fauna from the northern Ural region): Trudy Paleontologicheskogo Instituta Akademiya Nauk SSSR, v. 62, p. 5–50. [in Russian]

Kuhn, O., 1961, Die Familien der Rezenten und Fossilen Amphibien und Reptilien: Bamberg, Meisenbach-Verlag.

Langston, W. Jr., 1953, Permian amphibians from New Mexico: University of California Publications in Geological Sciences, v. 29, p. 349–416.

Laurin, M, and Soler-Gijón, R., 2001, The oldest stegocephalian from the Iberian Peninsula: evidence that temnospondyls were euryhaline: Comptes Rendus Academie des Sciences de la Vie, v. 324, p. 495–501.

Laurin, M. and Soler-Gijón, R., 2006, The oldest known stegocephalian (Sarcopterygii: Temnospondyli) from Spain: Journal of Vertebrate Paleontology, v. 26, p. 284–299.

Linnaeus, C., 1758, Systema naturae per regna tria naturae, secundum classes, ordines, genera, species, cum characteribus, differentiis, synonymis, locis, 10th ed.: Stockholm, Sweden, L. Salvii, p. 1–823.

Lydekker, R., 1889, Note on the occurrence of a species of *Bothriceps* in the Karroo System of South Africa: Annals and Magazine of Natural History, v. 4, p. 475–476.

Maddison, W.P., and Maddison, D.R., 1992, MacClade: analysis of phylogeny and character evolution: Sunderland, UK, Sinauer.

Menning, M., Glodny, J., Boy, J., Gast, R., Kowalczyk, G., Martens, T., Rößler, R., Schindler, T., von Seckendorff, V., and Voigt, S., 2022, The Rotliegend in the stratigraphic table of Germany 2016 (STG 2016): Zeitschrift der Deutschen Gesellschaft für Geowissenschaften, v. 173, p. 3–139.

Meyer, H. von, 1856, *Osteophorus Roemeri*: Jahrbuch für Mineralogie, Geologie und Paläontologie, v. 1856, p. 824.

Meyer, H. von, 1857, Über fossile Saurierknochen des orenburgischen Gouvernements: Neues Jahrbuch für Geognosie, Geologie und Petrefaktenkunde, v. 1857, p. 539–543.

Meyer, H. von, 1860a, *Osteophorus römeri* aus dem Rothliegenden von Klein Neundorf in Schlesien: Palaeontographica, v. 7, p. 99–104.

Meyer, H. von, 1860b, *Melosaurus uralensis* aus dem Permischen System des westlichen Urals: Palaeontographica, v. 7, p. 90–98.

Milner, A.R., 1989, The relationships of the eryopoid-grade temnospondyl amphibians from the Permian of Europe: Acta Musei Reginaehradecensis, v. 22, p. 131–137.

Milner, A.R., 1990, Chapter 15. The radiations of temnospondyl amphibians, *in* Taylor, P.D., and Larwood, G.P., eds., Major Evolutionary Radiations: Systematics Association Special Volume, v. 42, p. 321–349, Clarendon Press, Oxford, UK.

Milner, A.R., 1993, The Paleozoic relatives of lissamphibians: Herpetological Monographs, v. 7, p. 8–27.

Milner, A.R., and Sequeira, S.E.K., 1994, The temnospondyl amphibians from the Viséan of East Kirkton, West Lothian, Scotland: Transactions of the Royal Society of Edinburgh Earth Sciences, v. 84, p. 331–361.

Miner, R.W., 1925, The pectoral limb of *Eryops* and other primitive tetrapods: Bulletin of the American Museum of Natural History, v. 51, p. 145–312.

Moulton, J.M., 1974, A description of the vertebral column of *Eryops* based on the notes and drawings of A.S. Romer: Breviora, v. 428, p. 1–44.

Olson, E.C., 1958, Fauna of the Vale and Choza: 14. Summary, review, and integration of the geology and the faunas: Fieldiana, Geology, v. 10, p. 397–448.

Owen, R., 1853, Notes on the above-described fossil remains: Quarterly Journal of the Geological Society of London, v. 9, p. 66–67.

Pawley, K., 2006, The postcranial skeleton of temnospondyls (Tetrapoda: Temnospondyli) [Ph.D. Thesis]: Melbourne, La Trobe University, Department of Zoology, 470 p.

Pawley, K., and Warren, A.A., 2006, The appendicular skeleton of *Eryops megacephalus* Cope, 1877 (Temnospondyli: Eryopoidea) from the Lower Permian of North America: Journal of Paleontology, v. 80, p. 561–580.

Peters, G., 1991, Ordnung Crocodylia – krokodile, *in* Deckert, K., Deckert, G., Freytag, G.E., Günther, K., Peters, G., and Sterba, G., eds., Urania Tierreich: Fische, Lurche, Kriechtiere: Leipzig, Verlag, p. 519–529.

Quemeneur, S., de Buffrénil, V., and Laurin, M., 2013, Microanatomy of the amniote femur and inference of lifestyle in limbed vertebrates: Biological Journal of the Linnean Society, v. 109, p. 644–655.

Rinehart, L.F., and Lucas, S.G., 2013, Tooth form and function in temnospondyl amphibians: relationship of shape to applied stress: New Mexico Museum of Natural History and Sciences Bulletin, v. 61, p. 533–542.

Romer, A. S., 1928, Vertebrate faunal horizons in the Texas Permo-Carboniferous red beds: University of Texas Bulletin, v. 2801, p. 67–108.

https://doi.org/10.1017/jpa.2023.58 Published online by Cambridge University Press

Romer, A.S., 1947, Review of the Labyrinthodontia: Bulletin of the Museum of Comparative Zoology Harvard College, v. 99, p. 1–368.
Romer, A.S., 1952, Late Pennsylvanian and Early Permian vertebrates in the Pittsburgh–West Virginia region: Annals of Carnegie Museum, v. 33, p. 47–113.
Sanchez, S., Germain, D., de Ricqlès, A., Abourachid, A., Goussard, F., and Tafforeau, P., 2010, Limb-bone histology of temnospondyls: implications for understanding the diversification of palaeoecologies and patterns of locomotion of Permo-Triassic tetrapods: Journal of Evolutionary Biology, v. 23, p. 2076–2090.
Sander, P.M., 1987, Taphonomy of the Lower Permian Gerladine Bonebed in Archer County, Texas: Palaeogeography, Palaeoclimatology, Palaeoecology, v. 61, p. 221–236.
Sawin, H.J., 1941, The cranial anatomy of *Eryops megacephalus*: Bulletin of the Museum of Comparative Zoology, Harvard College, v. 88, p. 405–464.
Schäfer, A., 1986, Die sedimente des Oberkarbons und Unterrotliegenden im Saar–Nahe-Becken: Mainzer Geowissenschaftliche Mitteilungen, v. 15, p. 239–365.
Schneider, J.W., Lucas, S.G., Werneburg, R., and Rößler, R., 2010, Euramerican Late Pennsylvanian/Early Permian arthropleurid/tetrapod associations —implications for the habitat and paleobiology of the largest terrestrial arthropod: New Mexico Museum of Natural History and Science Bulletin, v. 49, p. 49–70.
Schneider, J.W., Lucas, S.G., Scholze, F., Voigt, S., Marchetti, L., et al., 2020, Late Paleozoic–early Mesozoic continental biostratigraphy—links to the standard global chronostratigraphic scale: Palaeoworld, v. 29, p. 186–238.
Schoch, R.R., 1997, Cranial anatomy of the Permian temnospondyl amphibian *Zatrachys serratus* Cope 1878, and the phylogenetic position of the Zatracheidae: Neues Jahrbuch für Geologie und Paläontologie, Abhandlungen, v. 206, p. 223–248.
Schoch, R.R., 2009a, Evolution of life cycles in early amphibians: Annual Review of Earth and Planetary Sciences, v. 37, p. 135–162.
Schoch, R.R., 2009b, Life-cycle evolution as response to diverse lake habitats in Paleozoic amphibians: Evolution, v. 63, p. 2738–2749.
Schoch, R.R., 2013, The evolution of major temnospondyl clades: an inclusive phylogenetic analysis: Journal of Systematic Palaeontology, v. 11, p. 673–705.
Schoch, R.R., 2014, Amphibian Evolution. The Life of Early Land Vertebrates: Chichester, UK, Wiley Blackwell, 264 p.
Schoch, R.R., 2021a, Osteology of the Permian temnospondyl amphibian *Glanochthon lellbachae* and its relationships: Fossil Record, v. 24, p. 49–64.
Schoch, R.R., 2021b, The life cycle in late Paleozoic eryopid temnospondyls: developmental variation, plasticity and phylogeny: Fossil Record, v. 24, p. 295–319.
Schoch, R.R., and Hampe, O., 2004, An eryopid-like temnospondyl from the Lower Rotliegend Meisenheim Formation of the Saar–Nahe Basin: Neues Jahrbuch für Geologie und Paläontologie, v. 232, p. 315–323.
Schoch, R.R., and Milner, A.R., 2014, Temnospondyli I, in Sues, H.-D., ed., Handbook of Paleoherpetology: Munich, Verlag Dr. Friedrich Pfeil, part 3A2, 150 p.
Schoch, R.R., and Seegis, D., 2016, A Middle Triassic palaeontological gold mine: the vertebrate deposits of Vellberg (Germany): Palaeogeography, Palaeoclimatology, Palaeoecology, v. 459, p. 249–267.
Schoch, R.R., and Sobral, G., 2021, A new species of *Sclerocephalus* with a fully ossified endocranium gives insight into braincase evolution in temnospondyls: Journal of Paleontology, v. 95, p. 1308–1320.
Schoch, R.R., and Voigt, S., 2019, A dvinosaurian temnospondyl from the Carboniferous-Permian boundary of Germany sheds light on dvinosaurian phylogeny and distribution: Journal of Vertebrate Paleontology, v. 39, https://doi.org/10.1080/02724634.2019.1577874.
Schoch, R.R., and Witzmann, F., 2009a, Osteology and relationships of the temnospondyl genus *Sclerocephalus*: Zoological Journal of the Linnean Society, v. 157, p. 135–168.
Schoch, R.R., and Witzmann, F., 2009b, The temnospondyl *Glanochthon* from the Lower Permian Meisenheim Formation of Germany: Special Papers in Palaeontology, v. 81, p. 121–136.
Sequeira, S.E., 2004, The skull of *Cochleosaurus bohemicus* Frič, a temnospondyl from the Czech Republic (Upper Carboniferous) and cochleosaurid interrelationships: Earth and Environmental Science Transactions of The Royal Society of Edinburgh, v. 94, p. 21–43.
Shelton, C.D., Sander, P.M., Stein, K., and Winkelhorst, H., 2013, Long bone histology indicates sympatric species of *Dimetrodon* (Lower Permian, Sphenacodontidae): Earth and Environmental Science Transactions of the Royal Society of Edinburgh, v. 103, p. 1–20.
Spindler, F., Voigt, S., and Fischer, J., 2020, Edaphosauridae (Synapsida, Eupelycosauria) from Europe and their relationship to North American representatives: PalZ, v. 94, p. 125–153.
Stapf, K.R.G., 1990, Einführung lithostratigraphischer Formationsnamen im Rotliegend des Saar–Nahe-Beckens (SW-Deutschland): Mitteilungen der Pollichia, v. 77, p. 111–124.
Steen, M.C., 1934, The amphibian fauna from the South Joggins, Nova Scotia: Proceedings of the Zoological Society of London, v. 1934, p. 465–504.
Swofford, D., 1991, PAUP: Phylogenetic Analysis Using Parsimony, Version 3.1: Champaign, Illinois, Illinois Natural History Survey.
Trautschold, H., 1884, Die reste Permischer Reptilien des paläontologischen kabinets der Universität Kasan: Nouveaux Memoires de la Societé Nationale Moscou, v. 15, p. 1–39.
Voigt, S., Fischer, J., Schindler, T., Wuttke, M., Spindler, F., and Rinehart, L., 2014, On a potential fossil hotspot for Pennsylvanian–Permian non-aquatic vertebrates in central Europe: Freiberger Forschungshefte, v. C548, p. 39–44.
Voigt, S., Schindler, T, Thum, H., and Fischer, J., 2019, Field trip C2: Pennsylvanian–Permian of the Saar–Nahe Basin, SW Germany. 19th International Congress on the Carboniferous and Permian, Cologne, July 29–August 2, 2019 – Field Guides: Kölner Forum für Geologie und Paläontologie, v. 24, p. 217–250.
Voigt, S., Schindler, T., Tichomirowa, M., Käßner, A., Schneider, J.W., and Linnemann, U., 2022, First high-precision U-Pb age from the Pennsylvanian–Permian of the continental Saar–Nahe Basin, SW Germany: International Journal of Earth Sciences, v. 111, p. 2129–2147.
von Seckendorff, V., 2012, Der Magmatismus in und zwischen den spätvariscischen permokarbonen Sedimentbecken in Deutschland: Schriftenreihe der Deutschen Gesellschaft für Geowissenschaften, v. 61, p. 743–860.
von Zittel, K., 1888–1890, Handbuch der Paläontologie. 1. Abtheilung: Paläozoologie. 3rd vol. Vertebrata (Pisces, Amphibia, Reptilia, Aves): Berlin, Oldenburg.
Walmsley, C.F., Smits, P.D., Quayle, M. R., McCurry, M.R., Richards, H.S., Oldfield, C.C., Wroe, S., Clausen, P.D., and McHenry, C.R., 2013, Why the long face? The mechanics of mandibular symphysis proportions in crocodiles: PLoS ONE, v. 8, e53873, https://doi.org/10.1371/journal.pone.0053873.
Warren, A.A., 2007, New data on *Ossinodus pueri*, a stem tetrapod from the Early Carboniferous of Australia: Journal of Vertebrate Paleontology, v. 27, p. 850–862.
Werneburg, R., 1987, Schädelrest eines sehr großwüchsigen Eryopiden (Amphibia) aus dem Unterrotliegenden (Unterperm) des Thüringer Waldes: Veröffentlichungen des Naturhistorischen Museums Schleusingen, v. 2, p. 52–56.
Werneburg, R., 1989, Die Amphibienfauna der Manebacher Schichten (Unterrotliegendes, Unterperm) des Thüringer Waldes: Veröffentlichungen des Naturhistorischen Museums Schleusingen, v. 4, p. 55–68.
Werneburg, R., 1993, *Onchiodon* (Eryopidae, Amphibia) aus dem Rotliegend des Innersudetischen Beckens (Böhmen): Paläontologische Zeitschrift, v. 67, p. 343–355.
Werneburg, R., 1997, Der Eryopide *Onchiodon* (Amphibia) aus dem Rotliegend des Beckens von Autun (Frankreich): Freiberger Forschungsheft, v. C466, p. 167–181.
Werneburg, R., 2007, Der "Manebacher Saurier" – ein neuer großer Eryopide (*Onchiodon*) aus dem Rotliegend (Unter-Perm) des Thüringer Waldes: Veröffentlichungen Naturhistorisches Museum Schleusingen, v. 22, p. 3–40.
Werneburg, R., and Berman, D.S., 2012. Revision of the aquatic eryopid temnospondyl *Glaukerpeton avinoffi* Romer, 1952, from the Upper Pennsylvanian of North America: Annals of Carnegie Museum, v. 81, p. 45–72.
Werneburg, R., and Steyer, J.-S., 1999, Redescription of the holotype of *Actinodon frossardi* (Amphibian, Temnospondyli) from the Lower Rotliegend of the Autun Basin (Lower Permian, France): Geobios, v. 32, p. 599–607.
Werneburg, R., and Steyer, J.-S., 2002, Revision of *Cheliderpeton vranyi* Fritsch, 1877 (Amphibia, Temnospondyli) from the Lower Permian of Bohemia (Czech Republic): Paläontologische Zeitschrift, v. 76, p. 149–162.
Werneburg, R., Lucas, S., Schneider, J.W., and Rinehart, L.F., 2010, First Pennsylvanian *Eryops* (Temnospondyli) and its Permian record from New Mexico, *in* Lucas, S.G., Schneider, J.W., and Spielmann, J.A., eds., Carboniferous–Permian transition in Canõn del Cobre, northern New Mexico: New Mexico Museum of Natural History and Science Bulletin, v. 49, p. 129–135.
Werneburg, R., Štamberg, S., and Steyer, J.-S., 2020, A new stereospondylomorph, *Korkonterpeton kalnense* gen. et sp. nov., from lower Permian of the Czech Krkonoše Piedmont Basin and a redescription of *Intasuchus silvicola* from the lower Permian of Russia (Temnospondyli, Amphibia): Fossil Imprint, v. 76, p. 217–242.
Williston, S.W., 1899, Notes on the coraco-scapula of *Eryops* COPE: The Kansas University Quarterly, v. 8, p. 185–186.
Witzmann, F., 2005, Hyobranchial and postcranial ontogeny of the temnospondyl *Onchiodon labyrinthicus* (GEINITZ, 1861) from Niederhäslich (Döhlen Basin, Autunian, Saxony): Paläontologische Zeitschrift, v. 79, p. 479–492.
Witzmann, F., 2006, Cranial morphology and ontogeny of the Permo-Carboniferous temnospondyl *Archegosaurus decheni* Goldfuss, 1847 from the Saar–Nahe Basin, Germany: Earth and Environmental Science Transactions of the Royal Society of Edinburgh, v. 96, p. 131–162.
Witzmann, F., 2009, Cannibalism in a small growth stage of the Early Permian branchiosaurid *Apateon gracilis* (Credner, 1881) from Saxony: Fossil Record, v. 12, p. 7–11.
Witzmann, F., 2013, The stratigraphically oldest eryopoid temnospondyl from the Permo-Carboniferous Saar–Nahe Basin, Germany: Paläontologische Zeitschrift, v. 87, p. 259–267.

https://doi.org/10.1017/jpa.2023.58 Published online by Cambridge University Press

Witzmann, F., and Voigt, S., 2014, An *Eryops*-like interclavicle from the Early Permian of the Saar–Nahe Basin, and a discussion of temnospondyl interclavicle characters: Paläontologische Zeitschrift, v. 89, p. 449–458.

Witzmann, F., Schoch, R.R., and Milner, A.R., 2007, The origin of the Dissorophoidea – an alternative perspective: Journal of Vertebrate Paleontology, supplement, v. 27, p. 167A.

Yates, A.M., and Warren, A.A., 2000, The phylogeny of the 'higher' temnospondyls (Vertebrata: Choanata) and its implications for the monophyly and origins of the Stereospondyli: Zoological Journal of the Linnean Society, v. 128, p. 77–121.

Accepted: 2 August 2023

https://doi.org/10.1017/jpa.2023.58 Published online by Cambridge University Press